Electronic Supplementary Material (ESI) for Dalton Transactions.
This journal is © The Royal Society of Chemistry 2017

Supporting Information

Insertion Reactions of Small Unsaturated Molecules in N–B Bonds of Boron Guanidinates

Alberto Ramos,*[a] Antonio Antiñolo,*[b] Fernando Carrillo-Hermosilla,[b] Rafael Fernández-Galán,[b] María del Pilar Montero-Rama,[b] Elena Villaseñor,[b] Antonio Rodríguez-Diéguez,[c] Daniel García-Vivó[d]

[a] *Departamento de Química Inorgánica, Orgánica y Bioquímica, Instituto Regional de Investigación Científica Aplicada, Universidad de Castilla-La Mancha, Campus Universitario, E-13071 Ciudad Real, Spain.*

[b] *Departamento de Química Inorgánica, Orgánica y Bioquímica, Facultad de Ciencias y Tecnologías Químicas, Universidad de Castilla-La Mancha, Campus Universitario, E-13071 Ciudad Real, Spain.*

[c] *Departamento de Química Inorgánica, Facultad de Ciencias, Universidad de Granada, Avenida de la Fuente Nueva S/N, 18071 Granada, Spain.*

[d] *Departamento de Química Orgánica e Inorgánica/IUQOEM, Universidad de Oviedo, E-33071 Oviedo, Spain.*

Table S1. Temperature (K), concentrations (mol/L) and equilibrium constants (K_{eq}) for the isonitrile de-insertion reaction of compound **10** at different temperatures in C_6D_6 ($K_{eq} = \frac{[\mathbf{11}][CNAr]}{[\mathbf{4}]}$). [Internal standard: tetrakis(trimethylsilyl)silane (TKS); [TKS] = $1.44 \cdot 10^{-2}$ M].

T (K)	[**11**] (M)	[**4**] = [CNAr] (M)	K_{eq} (mol/L)	1/T (K^{-1})	Ln K_{eq}
298.15	0.025344	0.00864	0.00294545	0.00335402	-5.82749213
303.15	0.024912	0.011376	0.00519482	0.0032987	-5.26009315
313.15	0.020592	0.01512	0.0111021	0.00319336	-4.50062119
323.15	0.016992	0.020016	0.02357817	0.00309454	-3.74743402
333.15	0.009216	0.024336	0.06426225	0.00300165	-2.74478291
343.15	0.008064	0.027792	0.09578314	0.00291418	-2.34566857
353.15	0.004176	0.029088	0.20261297	0.00283166	-1.59645769

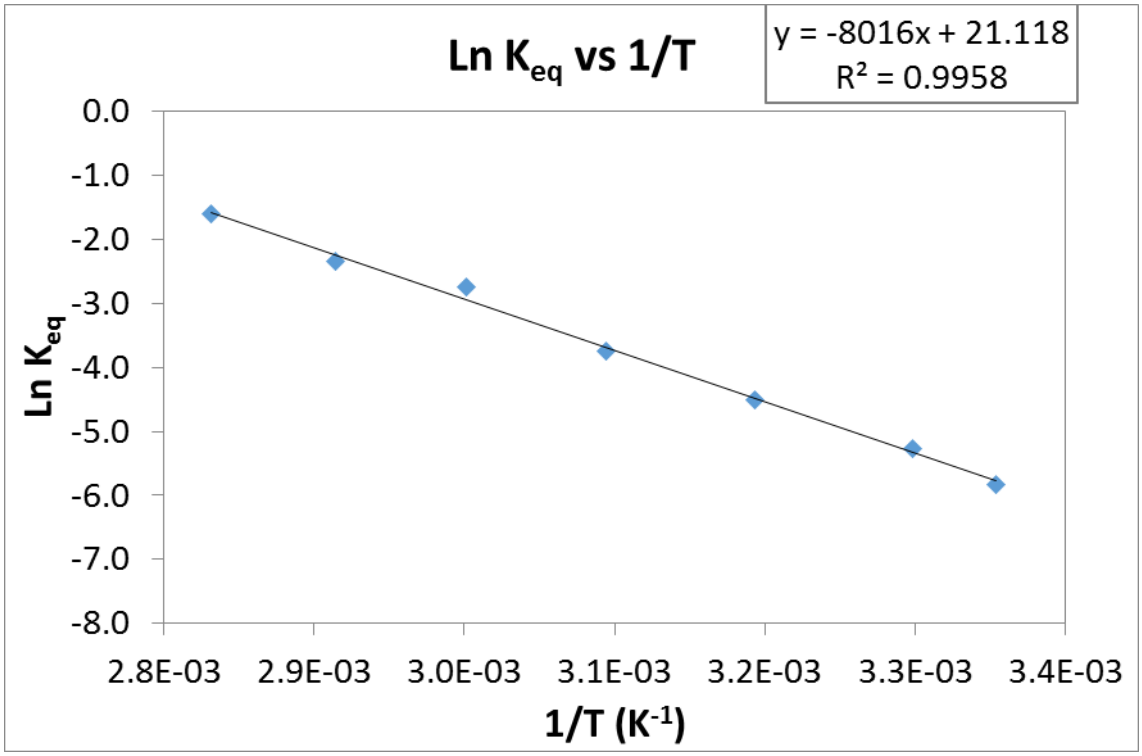

Figure S1. Van't Hoff plot (ln K_{eq} *vs* 1/T) for the isonitrile de-insertion reaction of compound **11.** ΔH^o = 66.6 ± 1.9 KJ mol^{-1}, ΔS^o = 175.6 ± 6.0 J mol^{-1} K^{-1}.

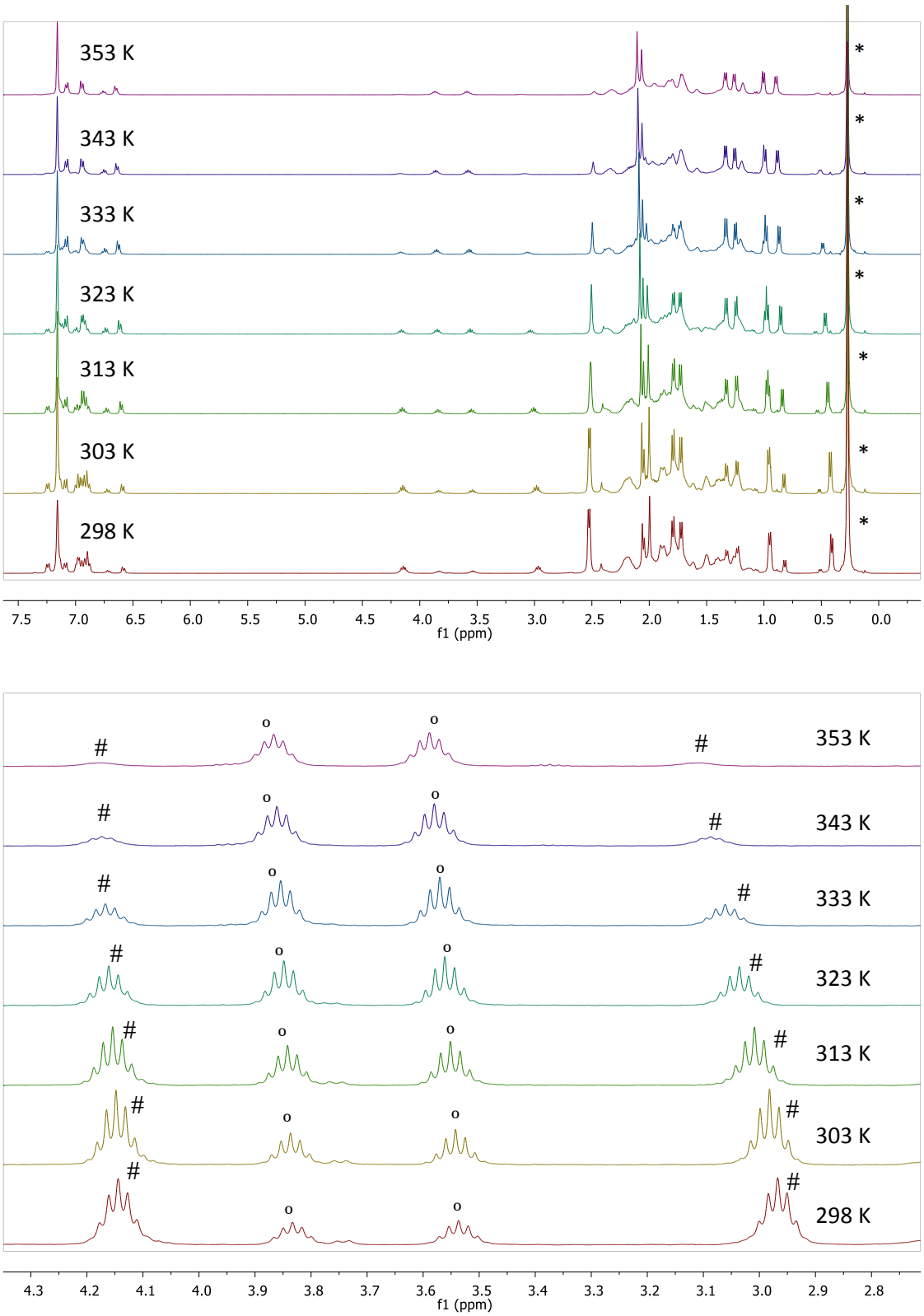

Figure S2. Stacked ^{1}H VT NMR spectra recorded in C_6D_6 at 400 MHz for the isonitrile de-insertion reaction of compound **11** (*top*: full spectra; *bottom*: C*H*-^{i}Pr area expanded; *TKS; # Compound **11**; ^{o} Compound **4**).

Table S2. Temperature (K), concentrations (mol/L) and equilibrium constants (K_{eq}) for the isonitrile de-insertion reaction of compound **10** at different temperatures in C_6D_6 ($K_{eq} = \frac{[\mathbf{12}][CNAr]}{[\mathbf{4}]}$). [Internal standard: tetrakis(trimethylsilyl)silane (TKS); [TKS] = $1.51 \cdot 10^{-2}$ M].

T (K)	[**12**] (M)	[**4**] = [CNAr] (M)	K_{eq} (mol/L)	1/T (K^{-1})	Ln K_{eq}
298.15	0.0334152	0.0025704	0.00019772	0.00335402	-8.52864311
303.15	0.0328104	0.003024	0.00027871	0.0032987	-8.1853399
313.15	0.0316008	0.0048384	0.00074081	0.00319336	-7.20776954
323.15	0.0305424	0.0077112	0.00194689	0.00309454	-6.24152353
333.15	0.0276696	0.0108864	0.00428317	0.00300165	-5.45306101
343.15	0.0232848	0.0140616	0.00849175	0.00291418	-4.76866071
353.15	0.0185976	0.0176904	0.01682745	0.00283166	-4.08474358

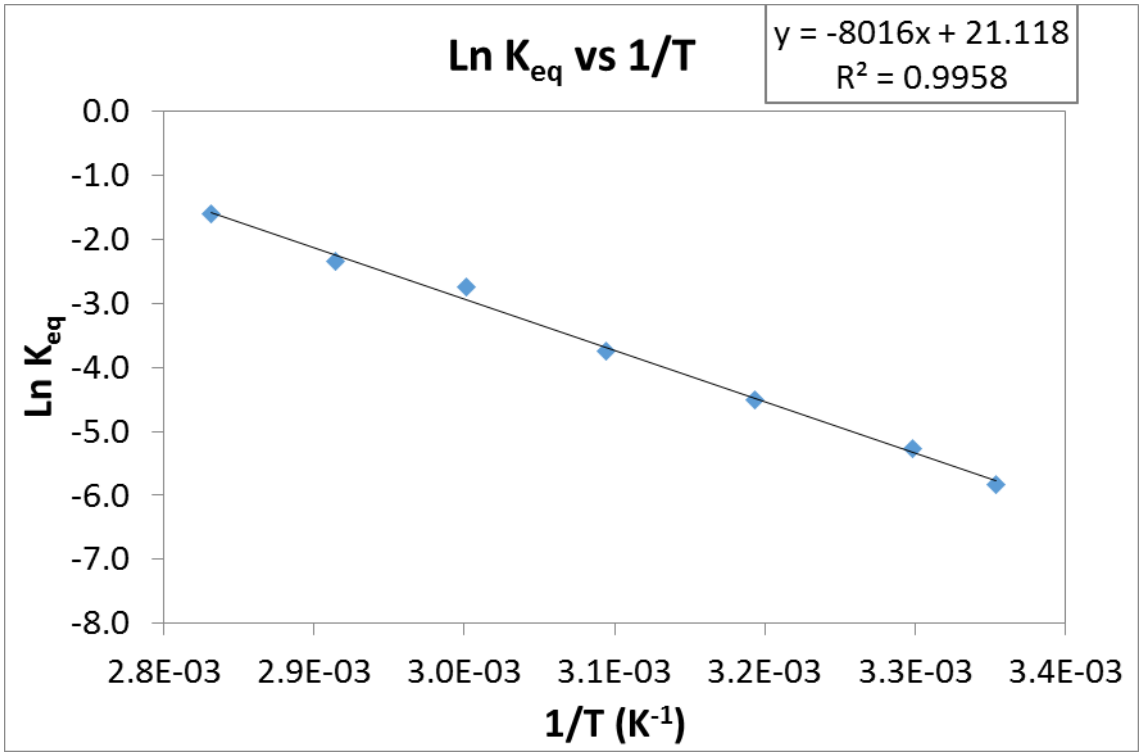

Figure S3. Van't Hoff plot (ln Keq vs 1/T) for the isonitrile de-insertion reaction of compound **12**. ΔH^o = 72.2 ± 1.2 KJ mol^{-1}, ΔS^o = 170.9 ± 3.7 J mol^{-1} K^{-1}.

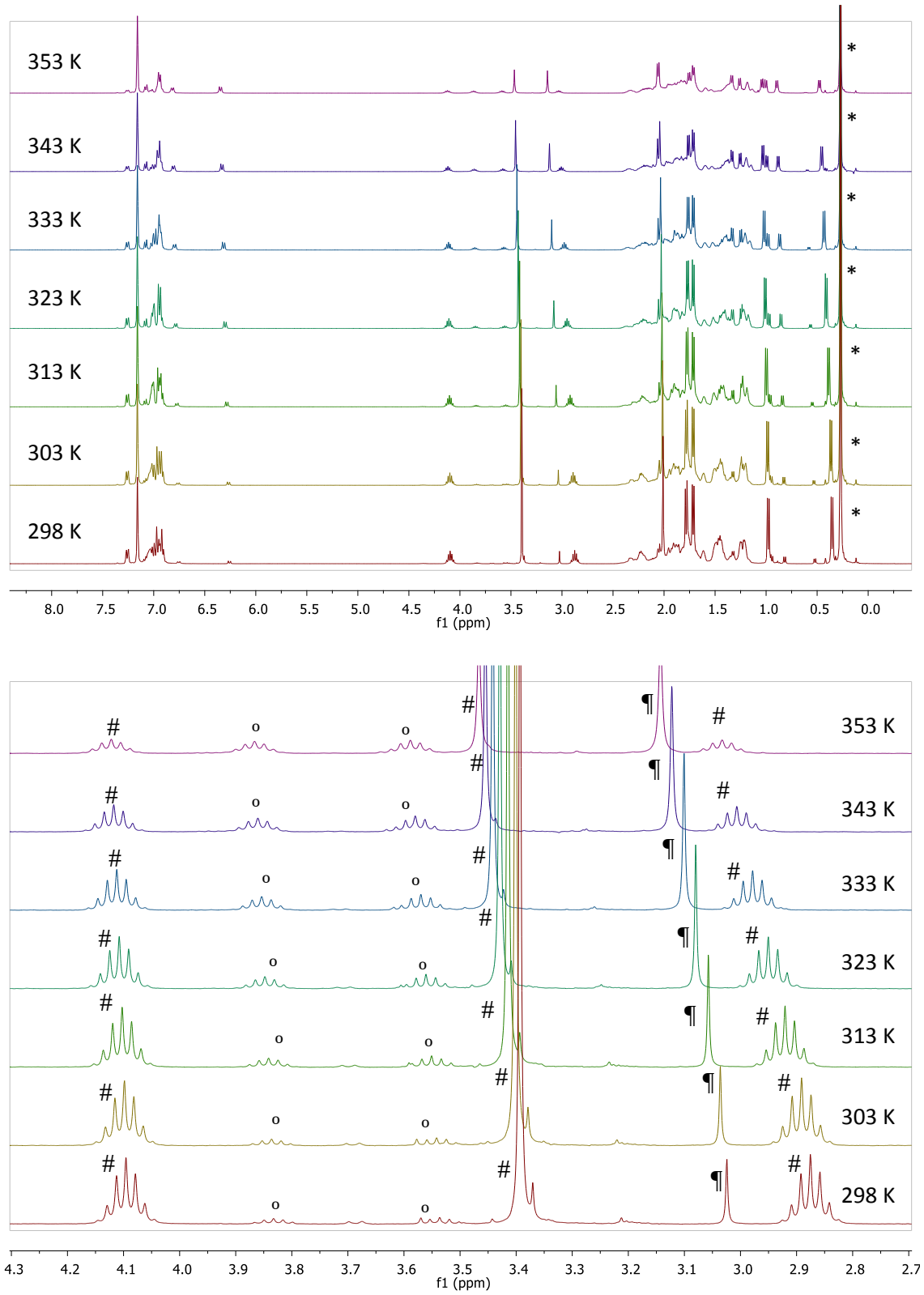

Figure S4. Stacked ^{1}H VT NMR spectra recorded in C_6D_6 at 400 MHz for the isonitrile de-insertion reaction of compound **12** [*top*: full spectra; *bottom*: C*H*-^{i}Pr and C*H*$_3$O area expanded; *TKS; # Compound **12**; º Compound **4**; ¶ CN(*p*-MeO-C_6H_4)].

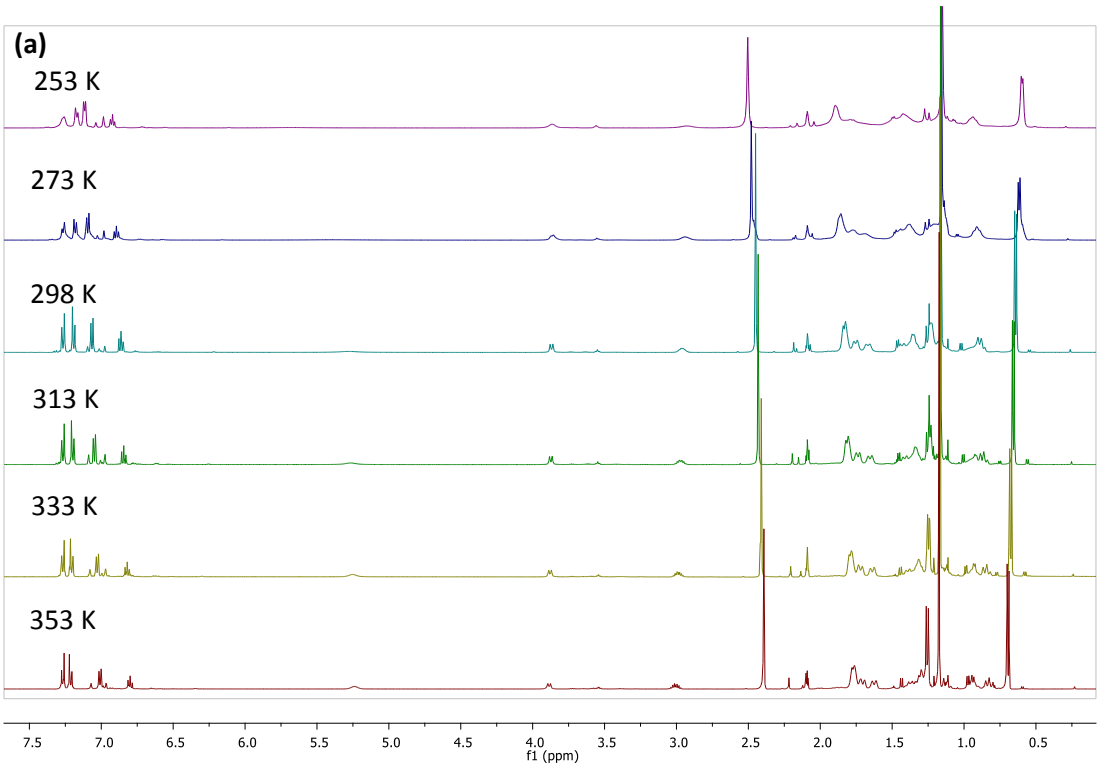
(a)
253 K
273 K
298 K
313 K
333 K
353 K
7.5 7.0 6.5 6.0 5.5 5.0 4.5 4.0 3.5 3.0 2.5 2.0 1.5 1.0 0.5
f1 (ppm)

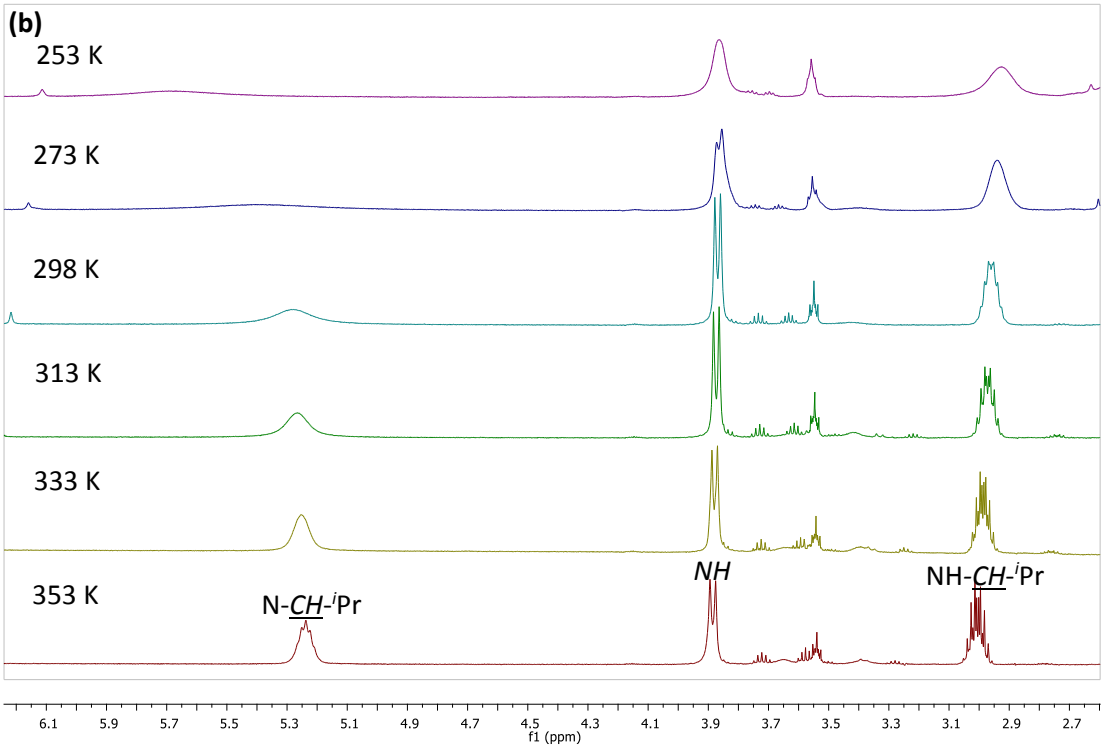
(b)
253 K
273 K
298 K
313 K
333 K
353 K
N-CH-iPr
NH
NH-CH-iPr
6.1 5.9 5.7 5.5 5.3 5.1 4.9 4.7 4.5 4.3 4.1 3.9 3.7 3.5 3.3 3.1 2.9 2.7
f1 (ppm)

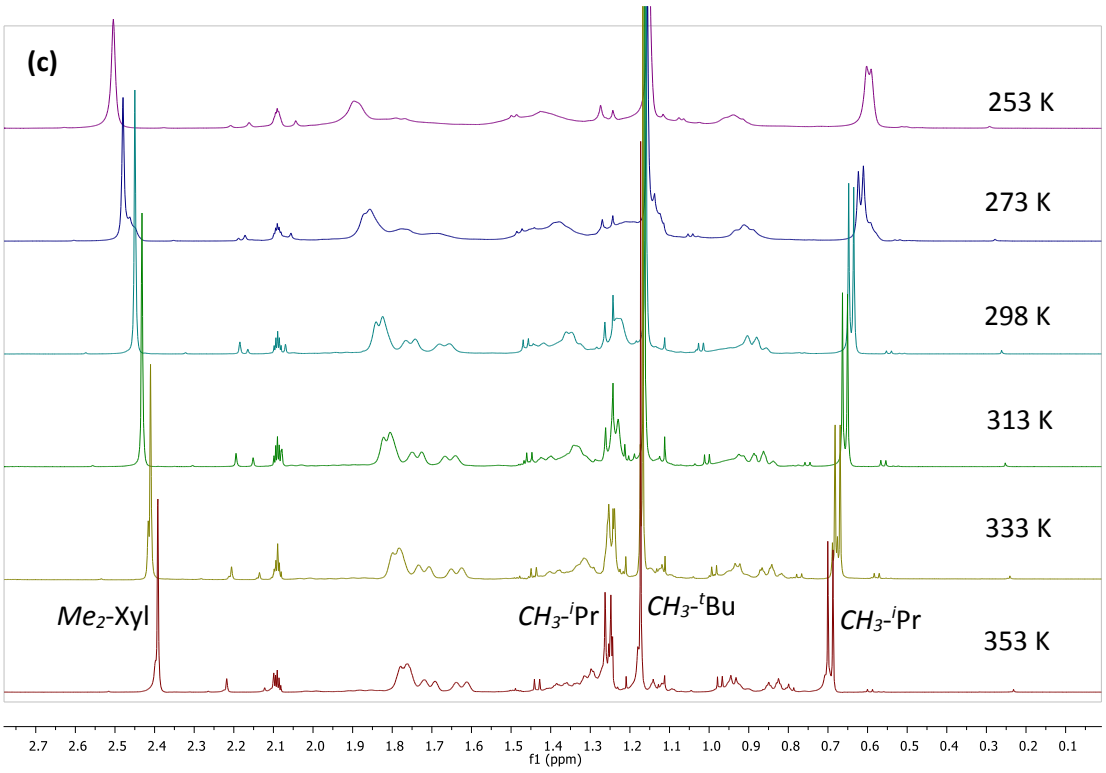

Figure S5. Stacked ^{1}H VT NMR spectra for compound **7a** in C_6D_6 at 500 MHz: (a) full spectra; (b) C*H*-^{i}Pr region expanded; (c) C*H*$_3$-^{i}Pr and *Me*$_2$-Xyl region expanded.

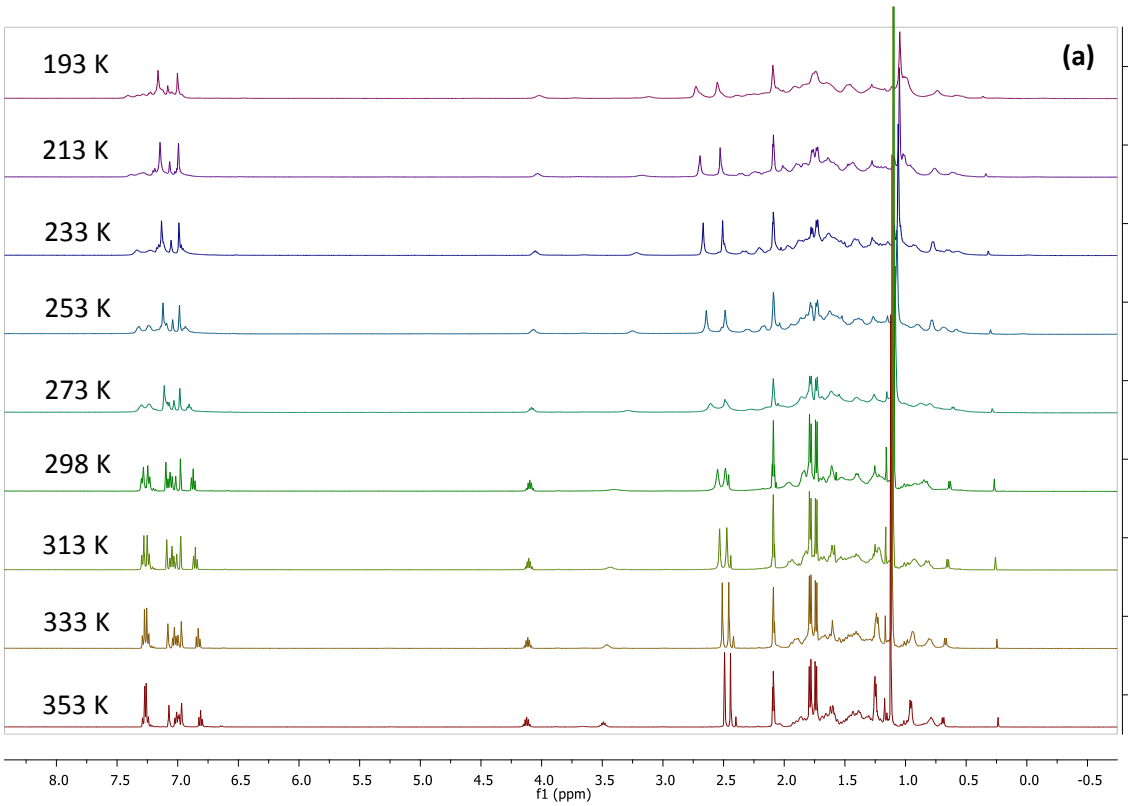
193 K
213 K
233 K
253 K
273 K
298 K
313 K
333 K
353 K
(a)
8.0 7.5 7.0 6.5 6.0 5.5 5.0 4.5 4.0 3.5 3.0 2.5 2.0 1.5 1.0 0.5 0.0 -0.5
f1 (ppm)

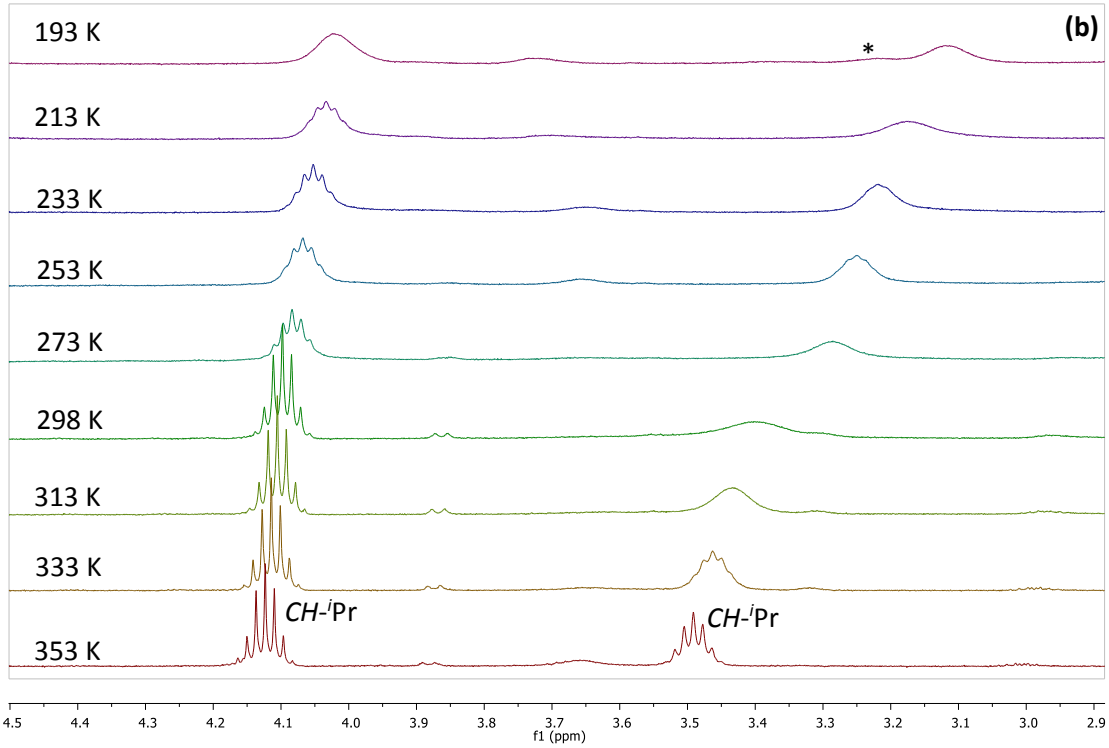
193 K
213 K
233 K
253 K
273 K
298 K
313 K
333 K
353 K
(b)
*
CH-iPr
CH-iPr
4.5 4.4 4.3 4.2 4.1 4.0 3.9 3.8 3.7 3.6 3.5 3.4 3.3 3.2 3.1 3.0 2.9
f1 (ppm)

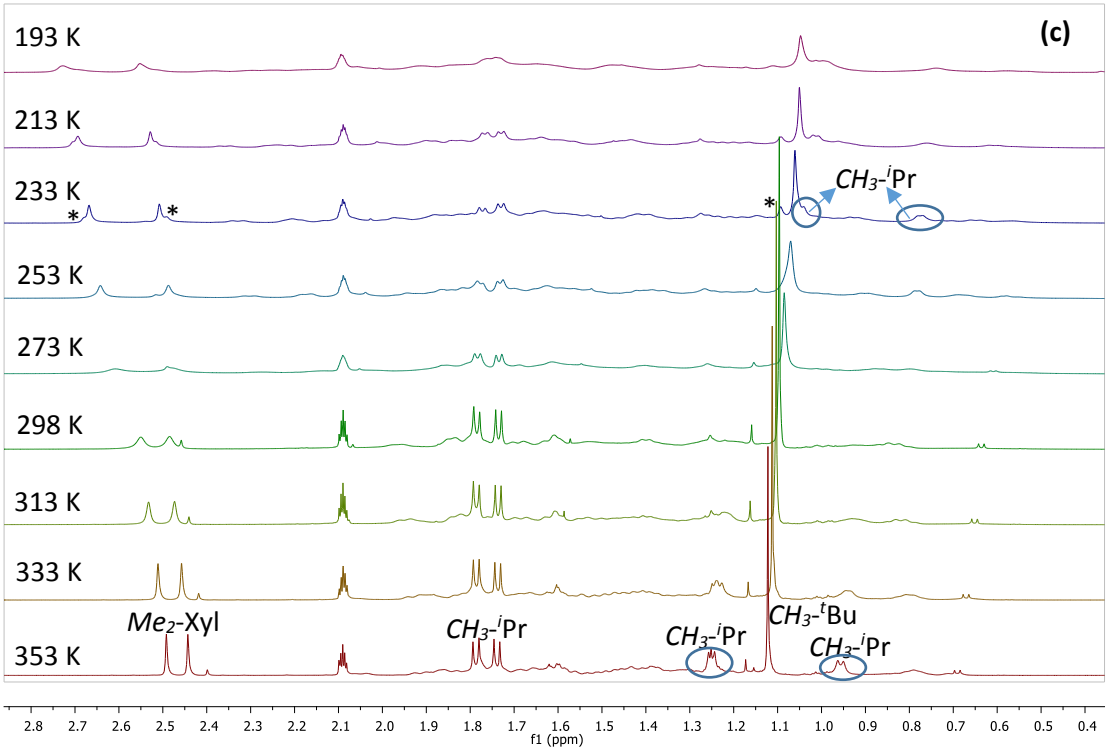

Figure S6. Stacked ^{1}H VT NMR spectra for compound **9** in C_6D_6 at 500 MHz: (a) full spectra; (b) C*H*-^{i}Pr region expanded; (c) C*H*$_3$-^{i}Pr and *Me*$_2$-Xyl region expanded. [* signals due to a minor rotamer].

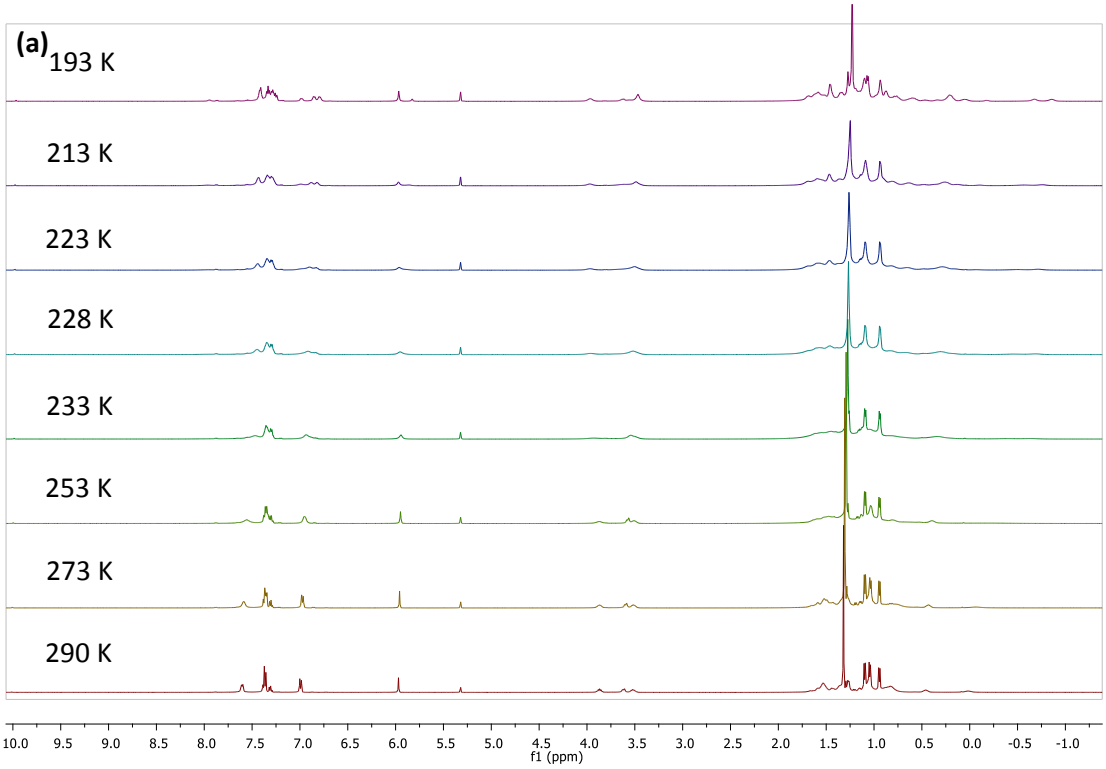
(a)
193 K
213 K
223 K
228 K
233 K
253 K
273 K
290 K
10.0 9.5 9.0 8.5 8.0 7.5 7.0 6.5 6.0 5.5 5.0 4.5 4.0 3.5 3.0 2.5 2.0 1.5 1.0 0.5 0.0 -0.5 -1.0
f1 (ppm)

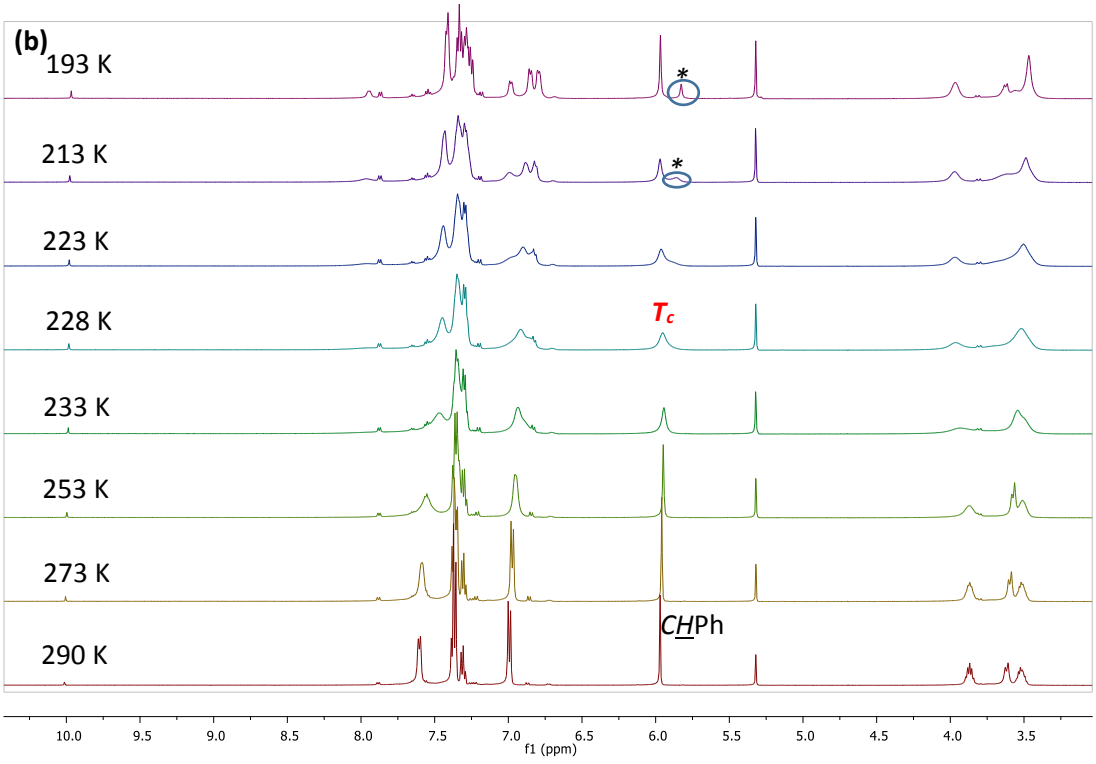
(b)
193 K
213 K
223 K
228 K
233 K
253 K
273 K
290 K
*
*
Tc
CHPh
10.0 9.5 9.0 8.5 8.0 7.5 7.0 6.5 6.0 5.5 5.0 4.5 4.0 3.5
f1 (ppm)

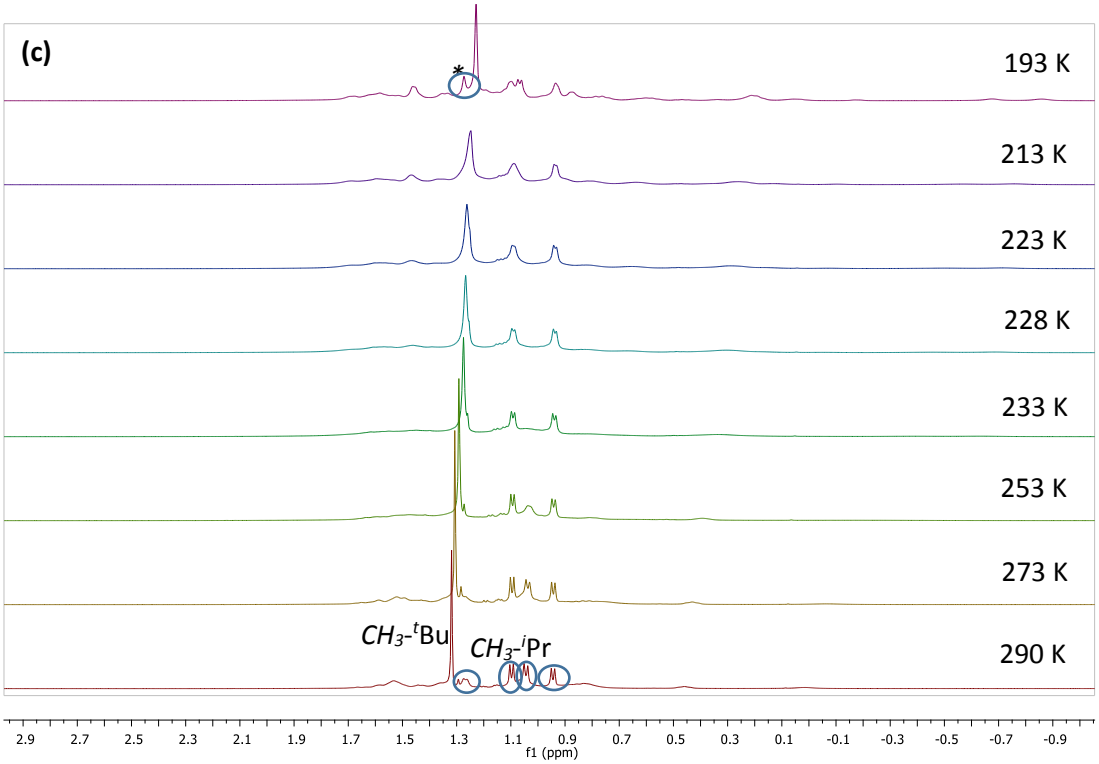

Figure S7. Stacked ^{1}H VT NMR spectra for compound **16a** in CD_2Cl_2 at 500 MHz: (a) full spectra; (b) 3 to 10 ppm region expanded; (c) −1 to 3 ppm region expanded. [* signals due to a minor rotamer].

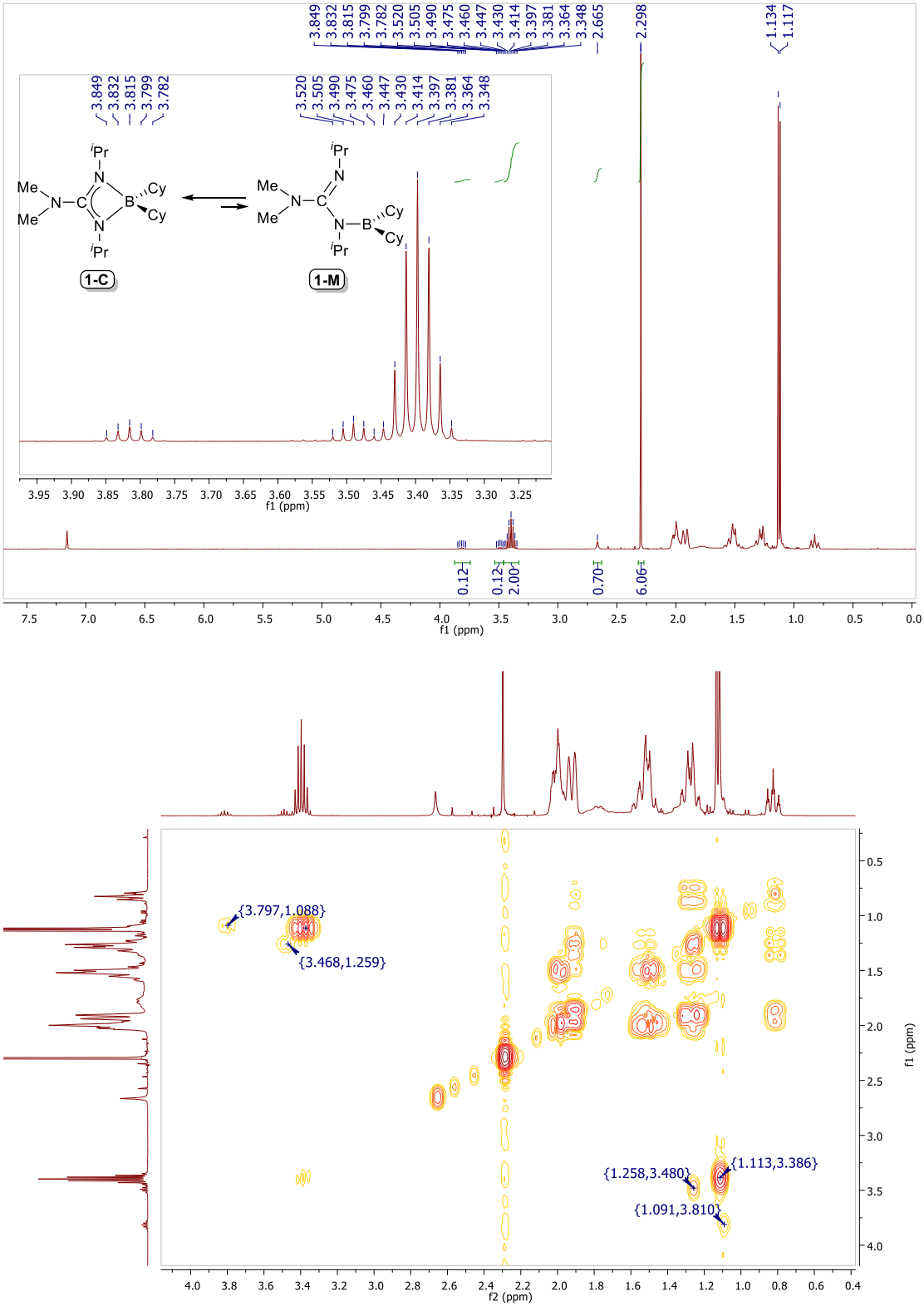

Figure S8. ^{1}H (top), ^{1}H-^{1}H COSY (bottom) NMR spectra for compound **1** in C_6D_6 (isomer mixture, **1-C** and **1-M**).

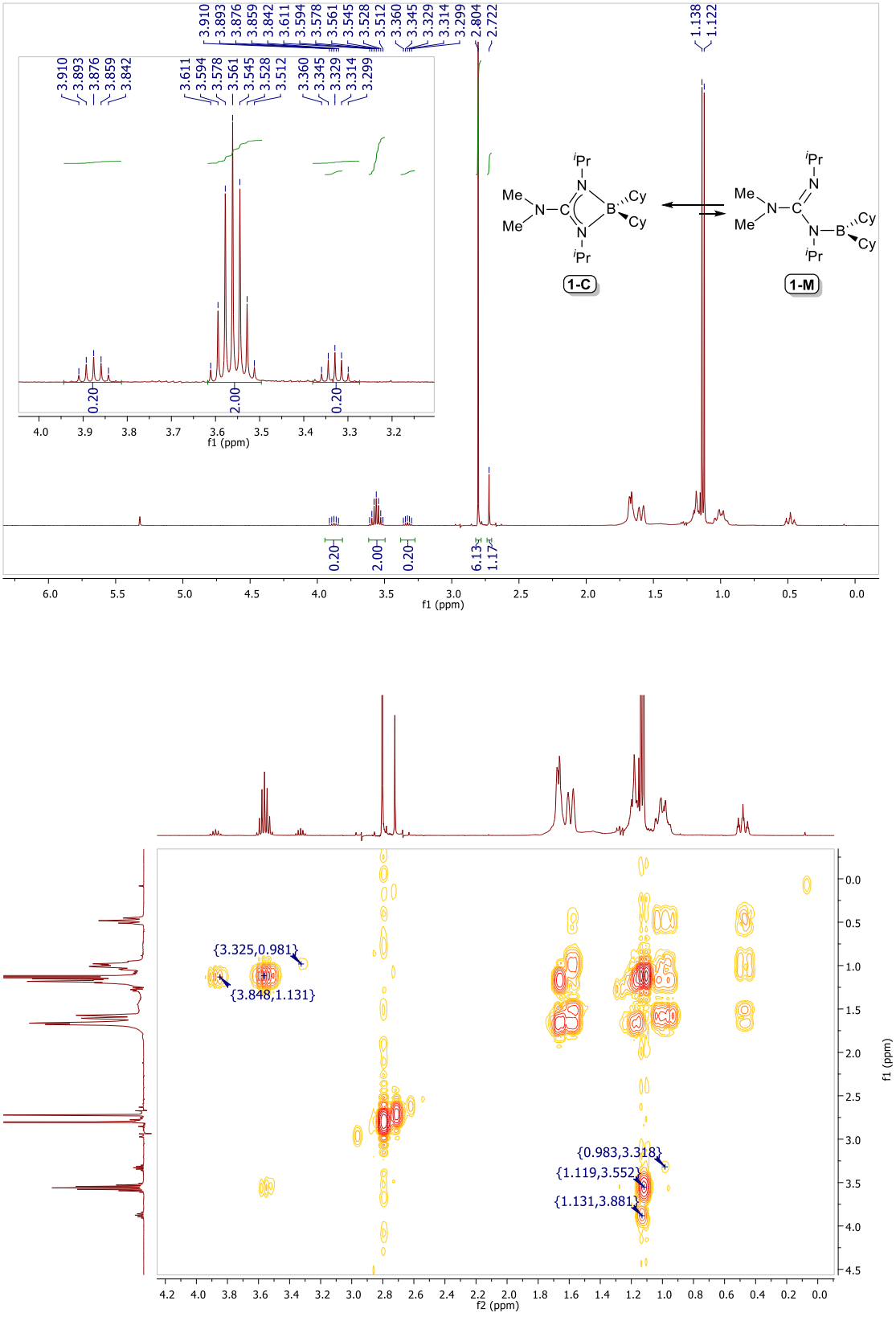

Figure S9. ^{1}H (top), ^{1}H-^{1}H COSY (bottom) NMR spectra for compound **1** in CD_2Cl_2 (isomer mixture, **1-C** and **1-M**).

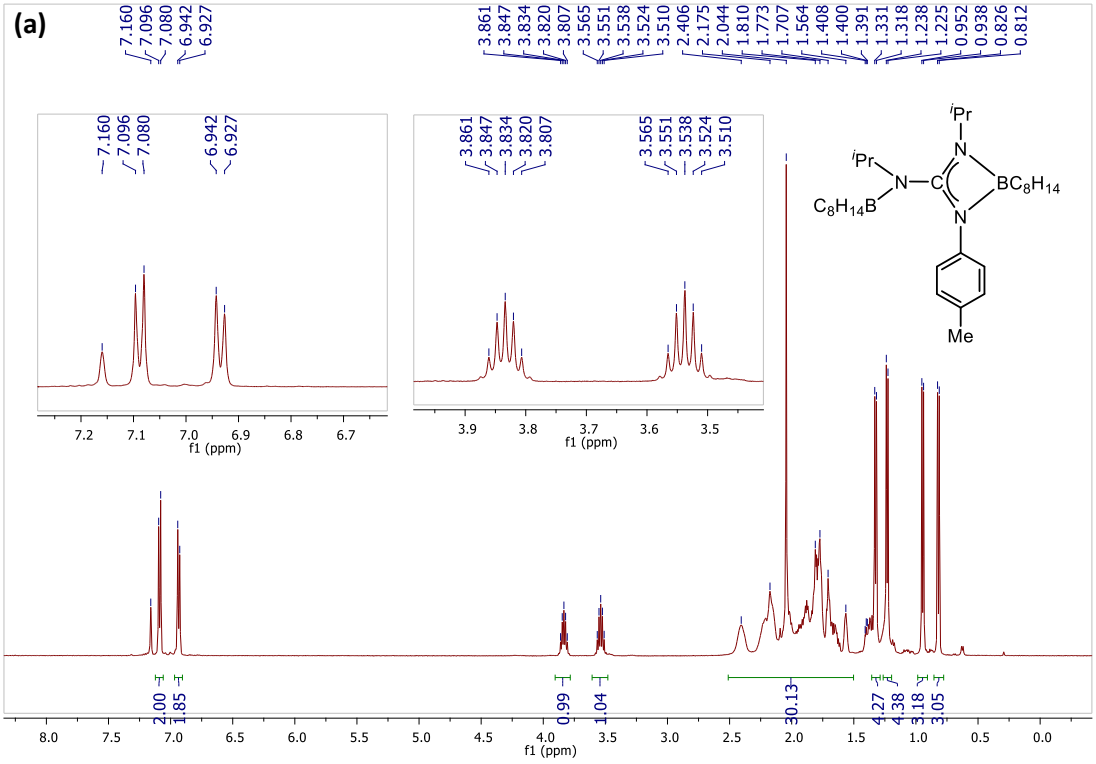
(a)
7.160
7.096
7.080
6.942
6.927
3.861
3.847
3.834
3.820
3.807
3.565
3.551
3.538
3.524
3.510
2.406
2.175
2.044
1.810
1.773
1.707
1.564
1.408
1.400
1.391
1.331
1.318
1.238
1.225
0.952
0.938
0.826
0.812
iPr
iPr
N
C
N
BC8H14
C8H14B
N
Me
2.00
1.85
0.99
1.04
30.13
4.27
4.38
3.18
3.05
f1 (ppm)

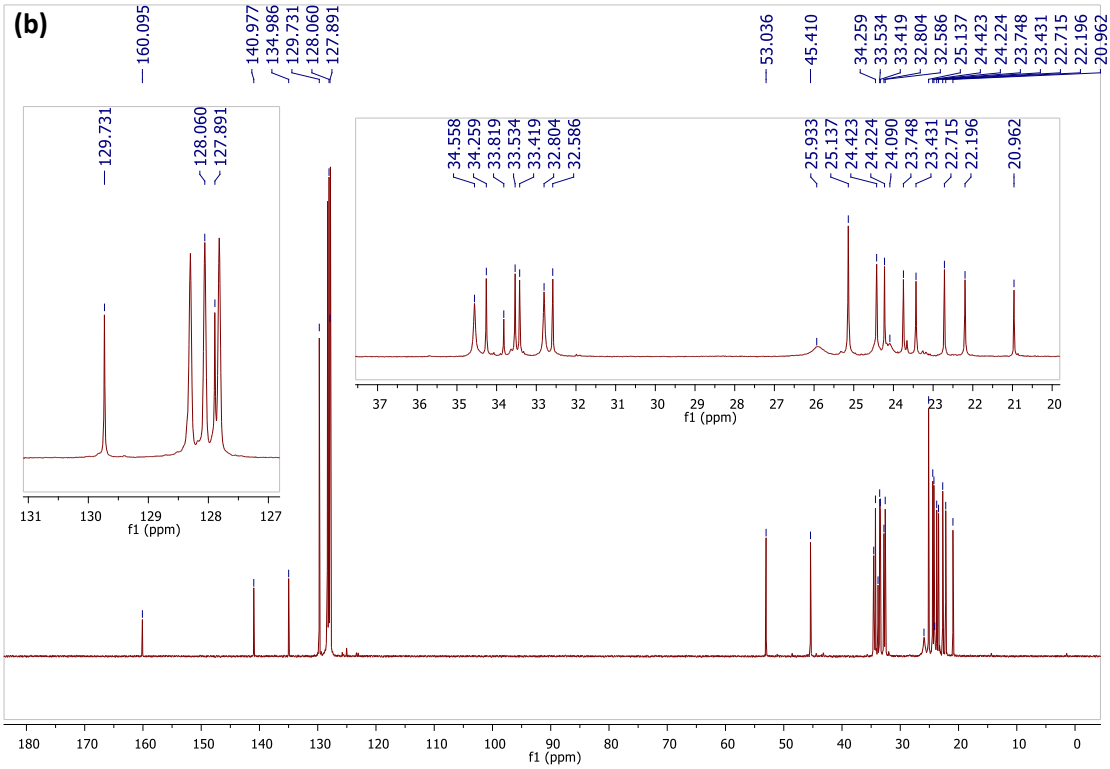
(b)
160.095
140.977
134.986
129.731
128.060
127.891
53.036
45.410
34.259
33.534
33.419
32.804
32.586
25.137
24.423
24.224
23.748
23.431
22.715
22.196
20.962
f1 (ppm)

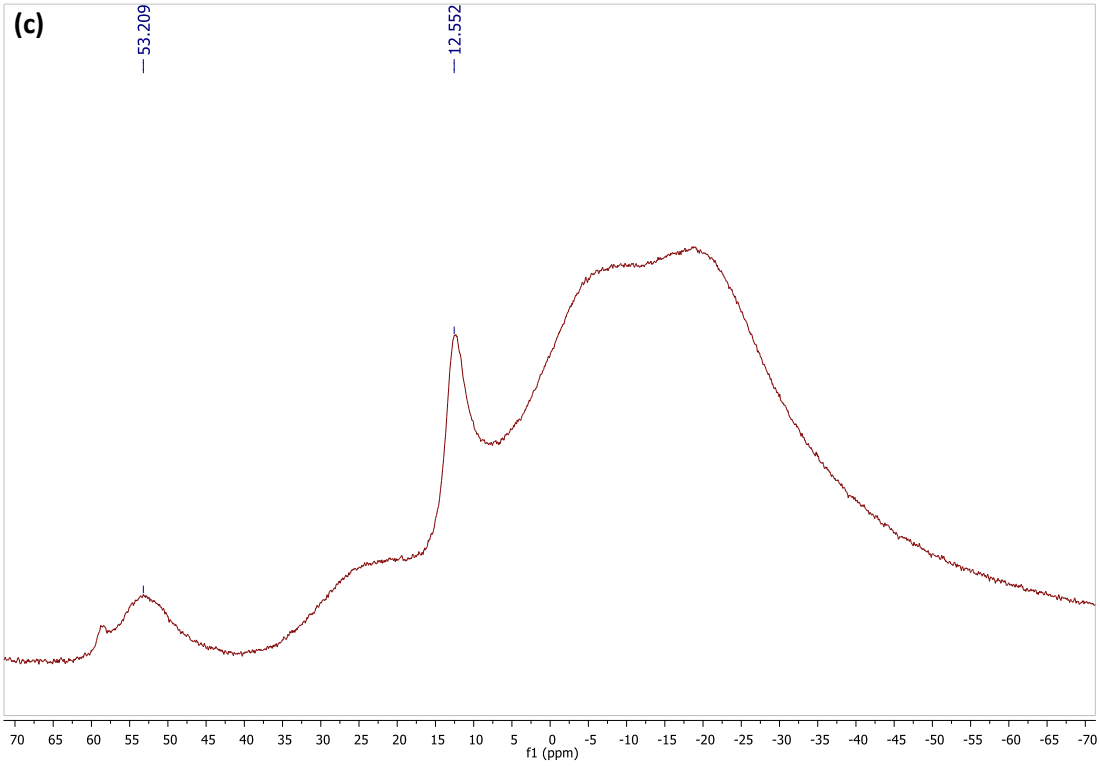

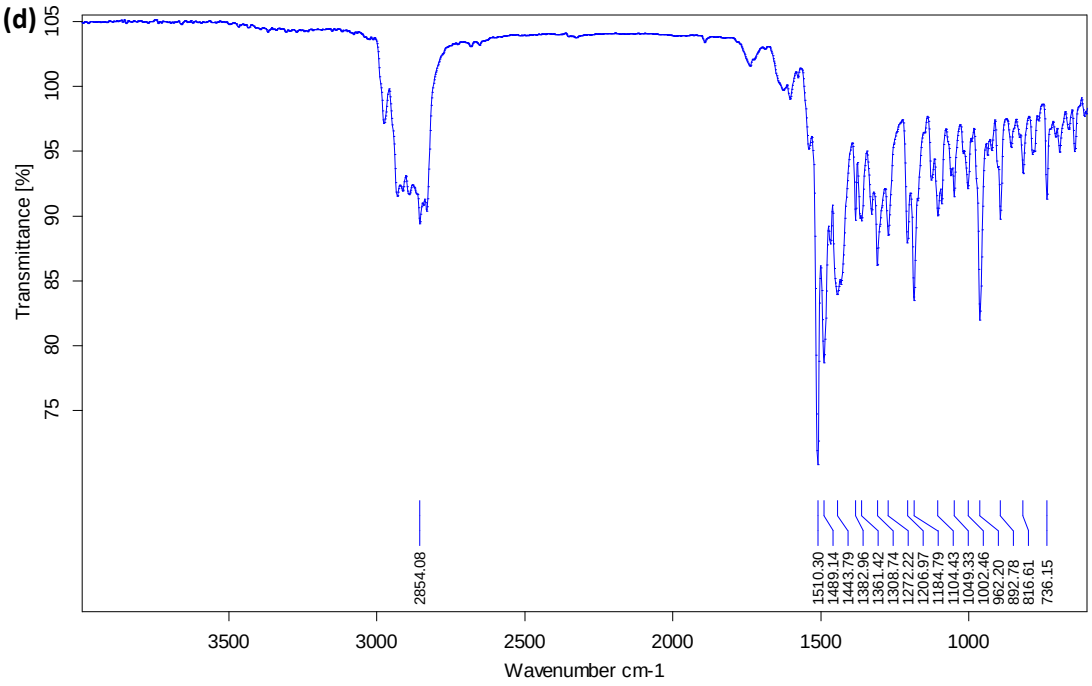

Figure S10. ^{1}H (a), $^{13}C\{^{1}H\}$ (b) and ^{11}B (c) NMR spectra in C_6D_6 solution, and ATR-IR spectrum (d) for compound **4**.

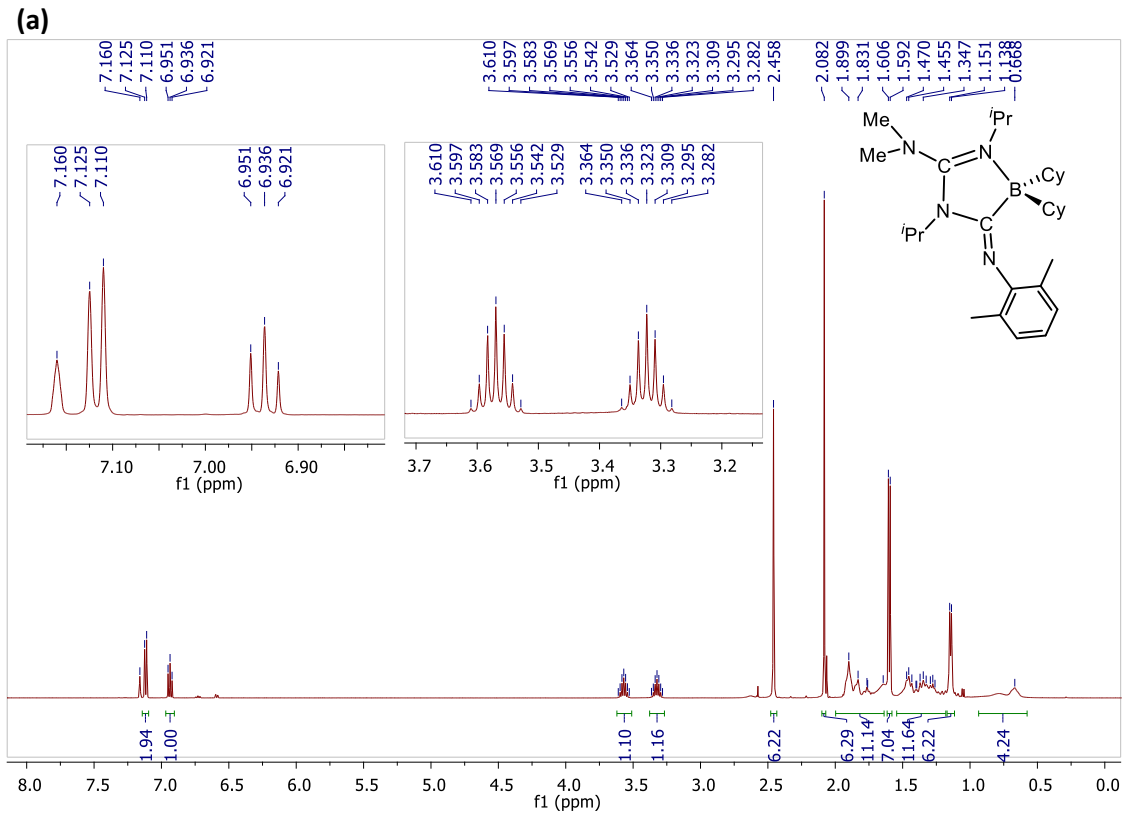
(a)
7.160
7.125
7.110
6.951
6.936
6.921
3.610
3.597
3.583
3.569
3.556
3.542
3.529
3.364
3.350
3.336
3.323
3.309
3.295
3.282
2.458
2.082
1.899
1.831
1.606
1.592
1.470
1.455
1.347
1.151
Me
Me
N
C
N
iPr
B
Cy
Cy
iPr
N
C
N
f1 (ppm)
1.94
1.00
1.10
1.16
6.22
6.29
11.14
7.04
11.64
6.22
4.24
f1 (ppm)

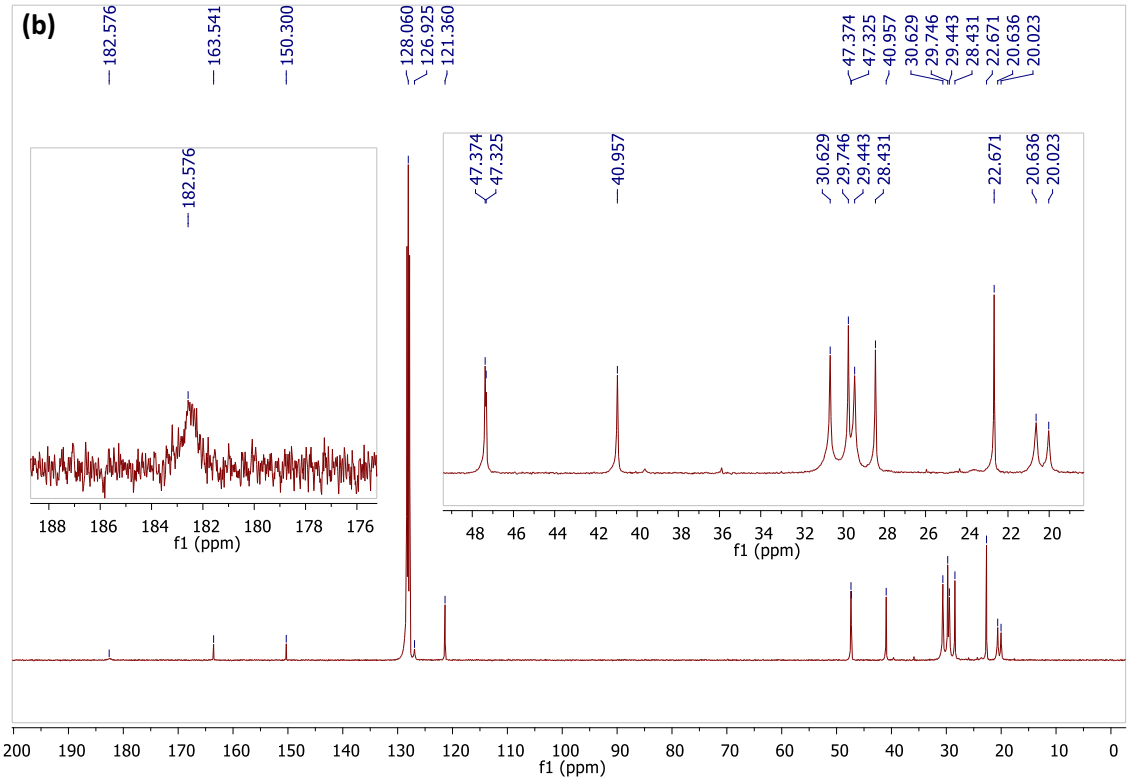
(b)
182.576
163.541
150.300
128.060
126.925
121.360
47.374
47.325
40.957
30.629
29.746
29.443
28.431
22.671
20.636
20.023
f1 (ppm)
f1 (ppm)
f1 (ppm)

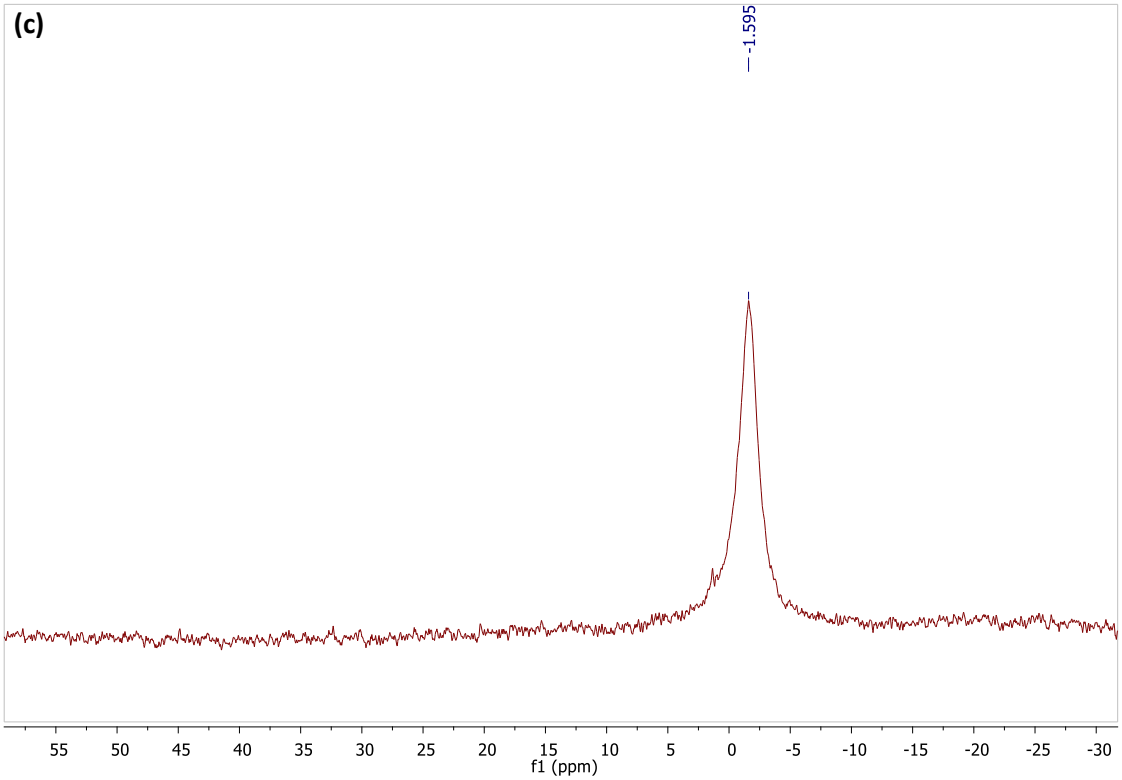

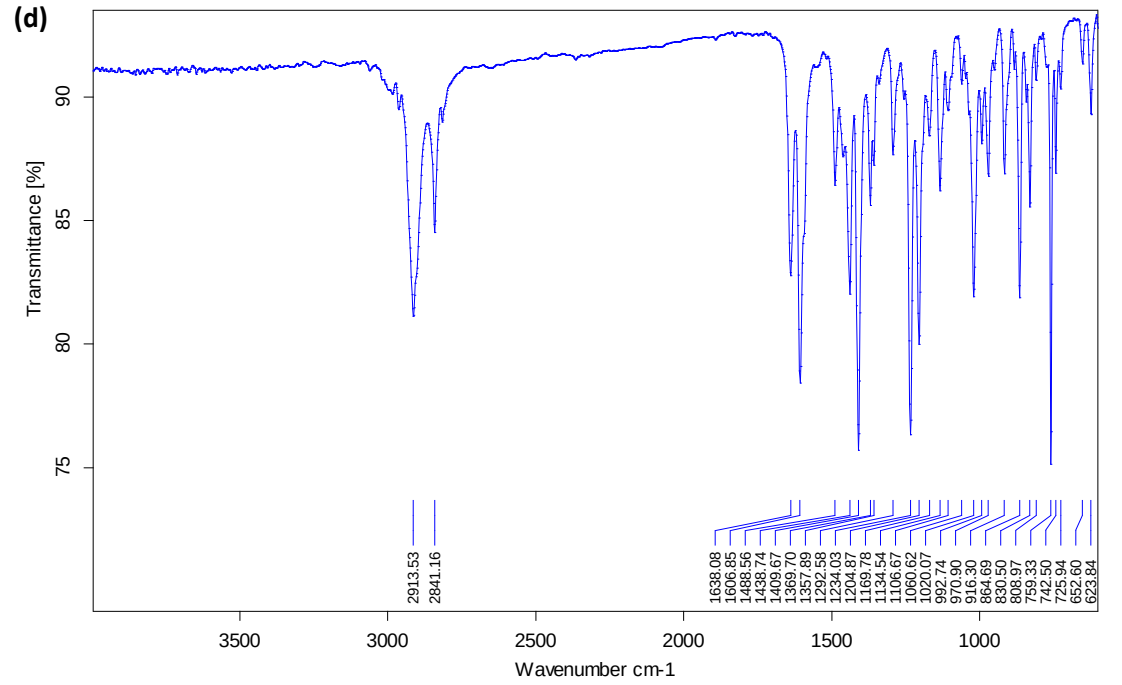

Figure S11. ^{1}H (a), $^{13}C\{^{1}H\}$ (b) and ^{11}B (c) NMR spectra in C_6D_6 solution, and ATR-IR spectrum (d) for compound **5**.

(a)

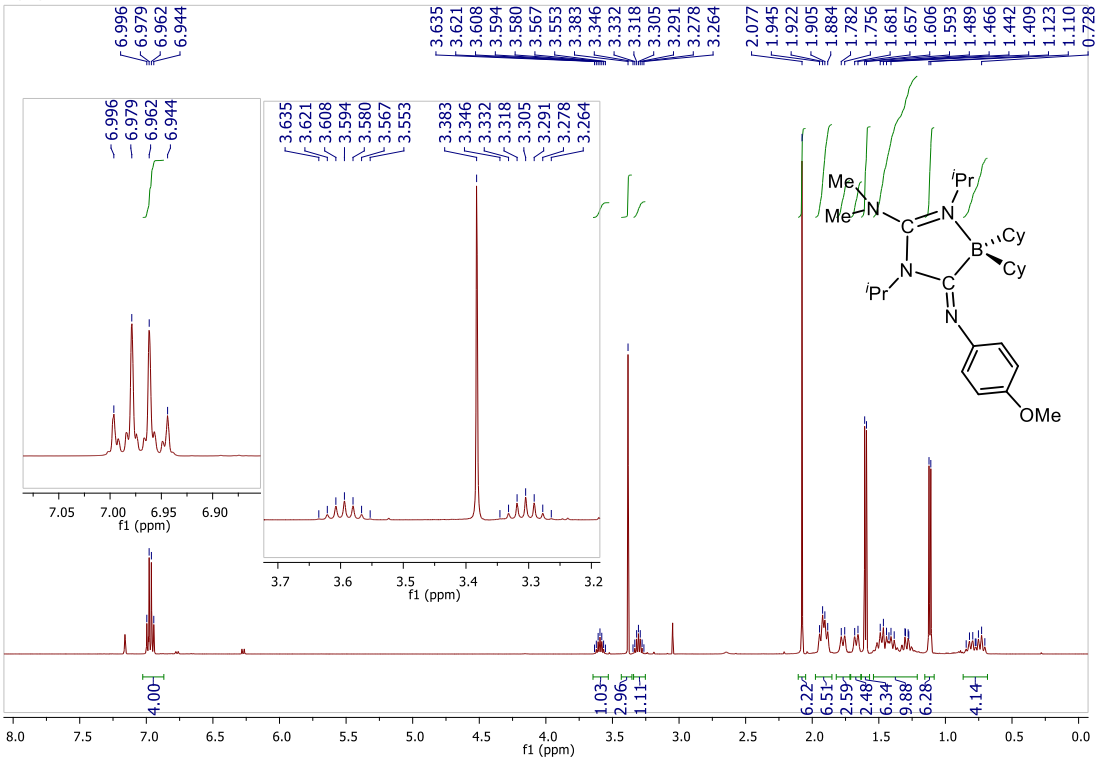
6.996
6.979
6.962
6.944
3.635
3.621
3.608
3.594
3.580
3.567
3.553
3.383
3.346
3.332
3.318
3.305
3.291
3.278
3.264
2.077
1.945
1.922
1.905
1.884
1.782
1.756
1.681
1.657
1.606
1.593
1.489
1.466
1.442
1.409
1.123
1.110
0.728
Me
Me
N
C
N
iPr
B
Cy
Cy
N
C
iPr
N
OMe
4.00
1.03
2.96
1.11
6.22
6.51
2.59
2.48
6.34
9.88
6.28
4.14
f1 (ppm)

(b)

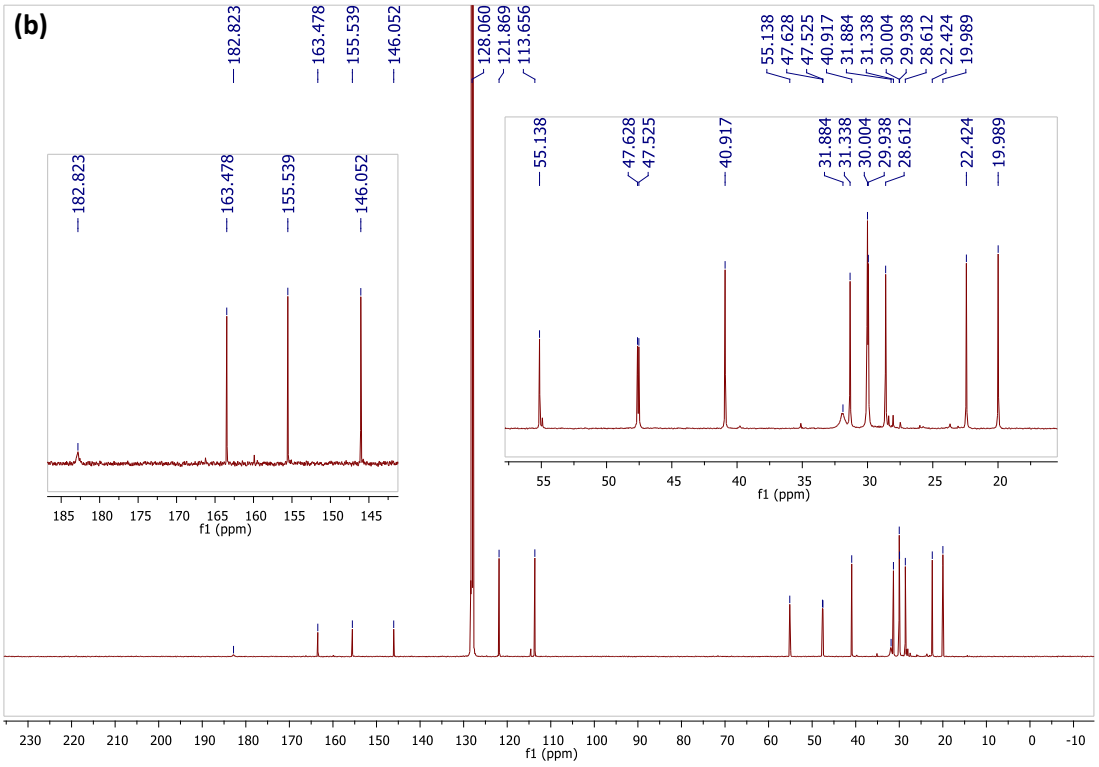
182.823
163.478
155.539
146.052
128.060
121.869
113.656
55.138
47.628
47.525
40.917
31.884
31.338
30.004
29.938
28.612
22.424
19.989
f1 (ppm)

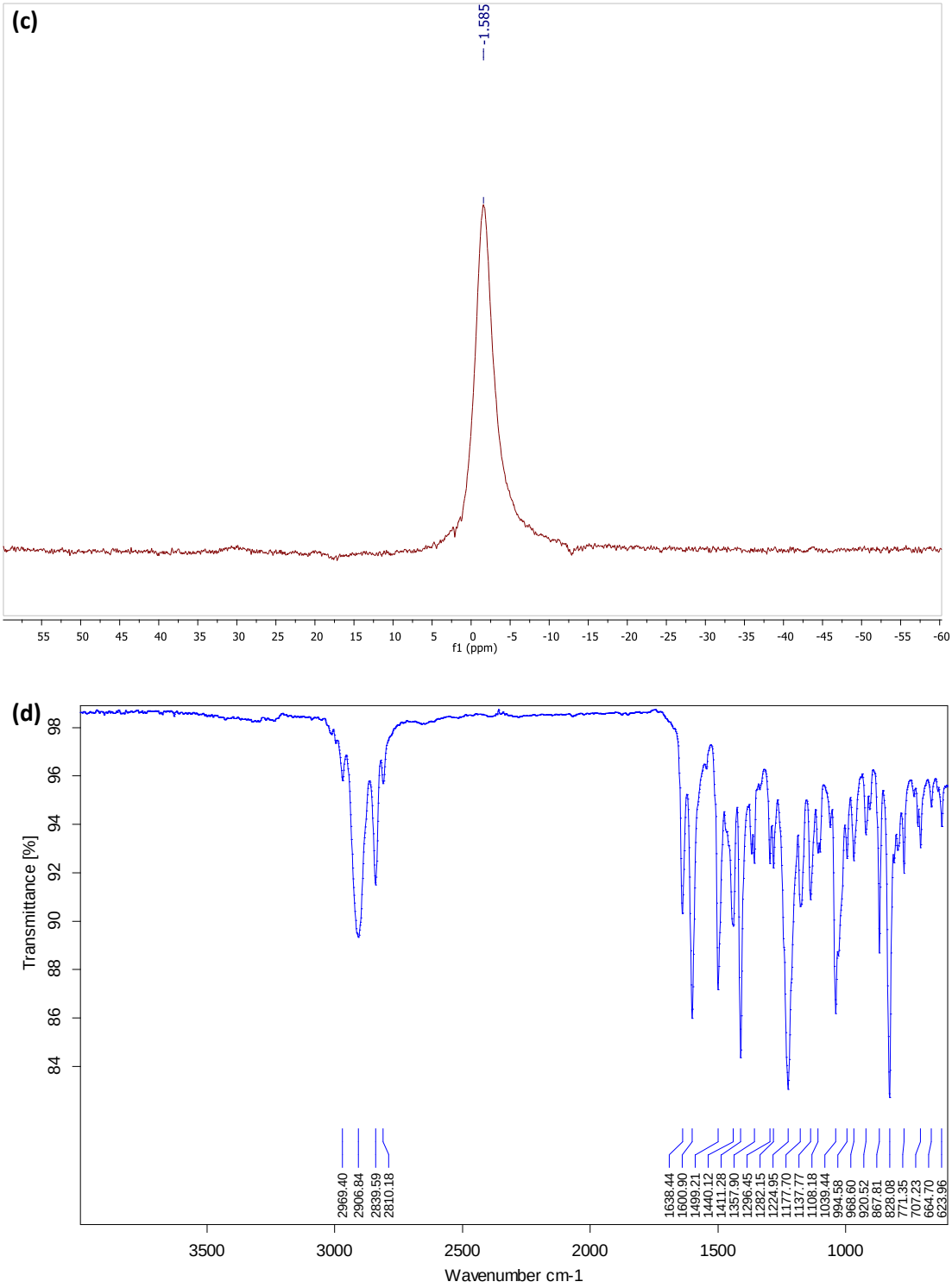

Figure S12. ^{1}H (a), $^{13}C\{^{1}H\}$ (b) and ^{11}B (c) NMR spectra in C_6D_6 solution, and ATR-IR spectrum (d) for compound **6**.

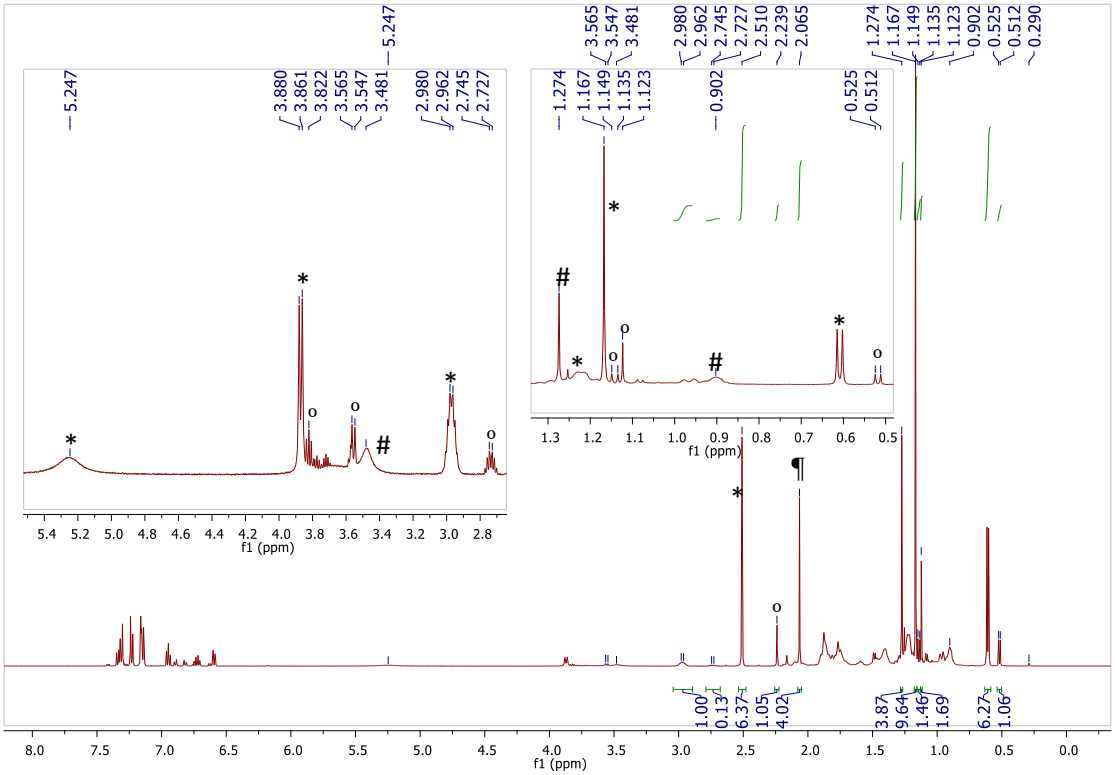

Figure S13. ^{1}H NMR spectrum in C_6D_6 solution at 298K of the reaction crude of **2** with CNXyl.* Compound **7a**; º Compound **7b**; ¶ CNXyl; # (*p*-Me-C_6H_4N)C(NH^{i}Pr)$_2$.

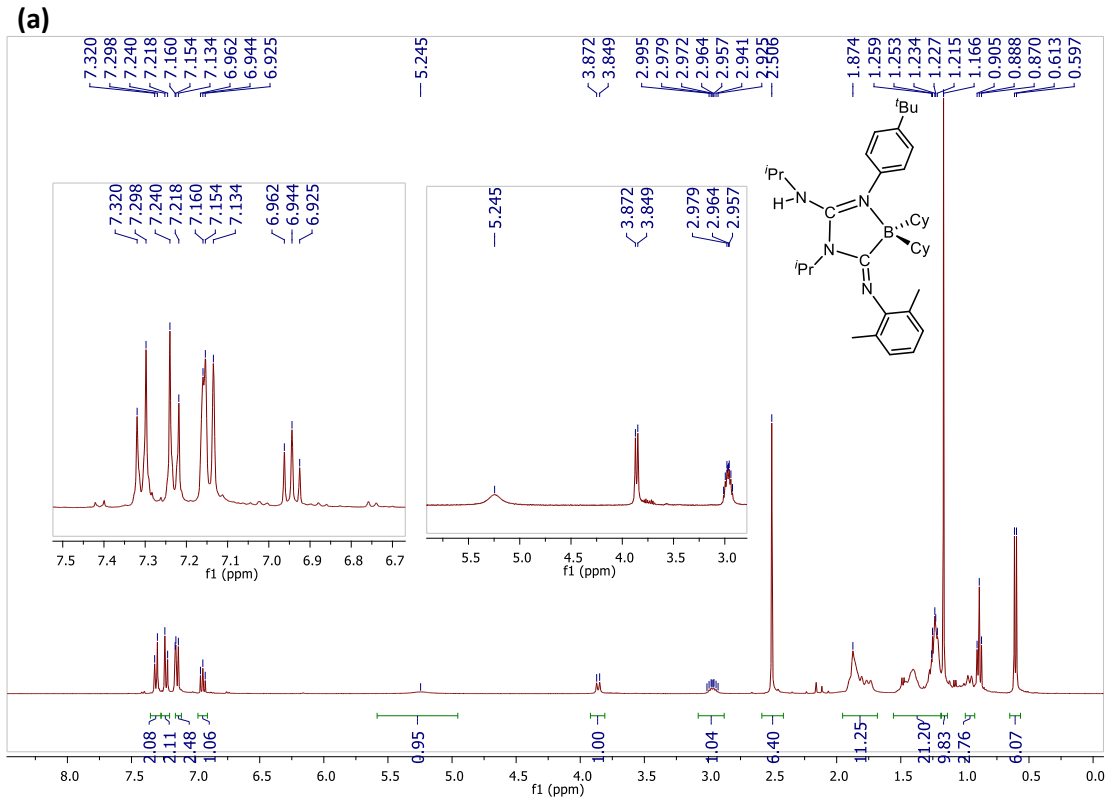
(a)
7.320
7.298
7.240
7.218
7.160
7.154
7.134
6.962
6.944
6.925
5.245
3.872
3.849
2.995
2.979
2.972
2.964
2.957
2.941
2.925
2.506
1.874
1.259
1.253
1.234
1.227
1.215
1.166
0.905
0.888
0.870
0.613
0.597
tBu
iPr
H
N
C
N
B
Cy
Cy
iPr
N
C
N
f1 (ppm)
2.08
2.11
2.48
1.06
0.95
1.00
1.04
6.40
11.25
21.20
9.83
2.76
6.07

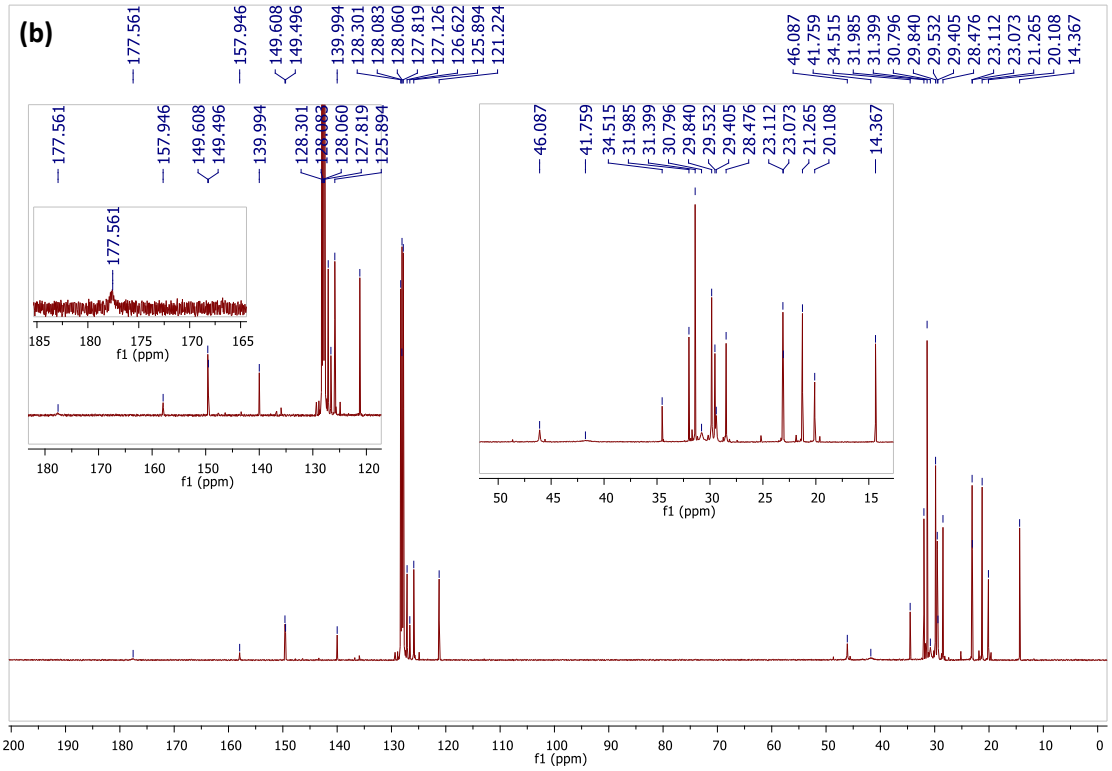
(b)
177.561
157.946
149.608
149.496
139.994
128.301
128.083
128.060
127.819
127.126
126.622
125.894
121.224
46.087
41.759
34.515
31.985
31.399
30.796
29.840
29.532
29.405
28.476
23.112
23.073
21.265
20.108
14.367
f1 (ppm)

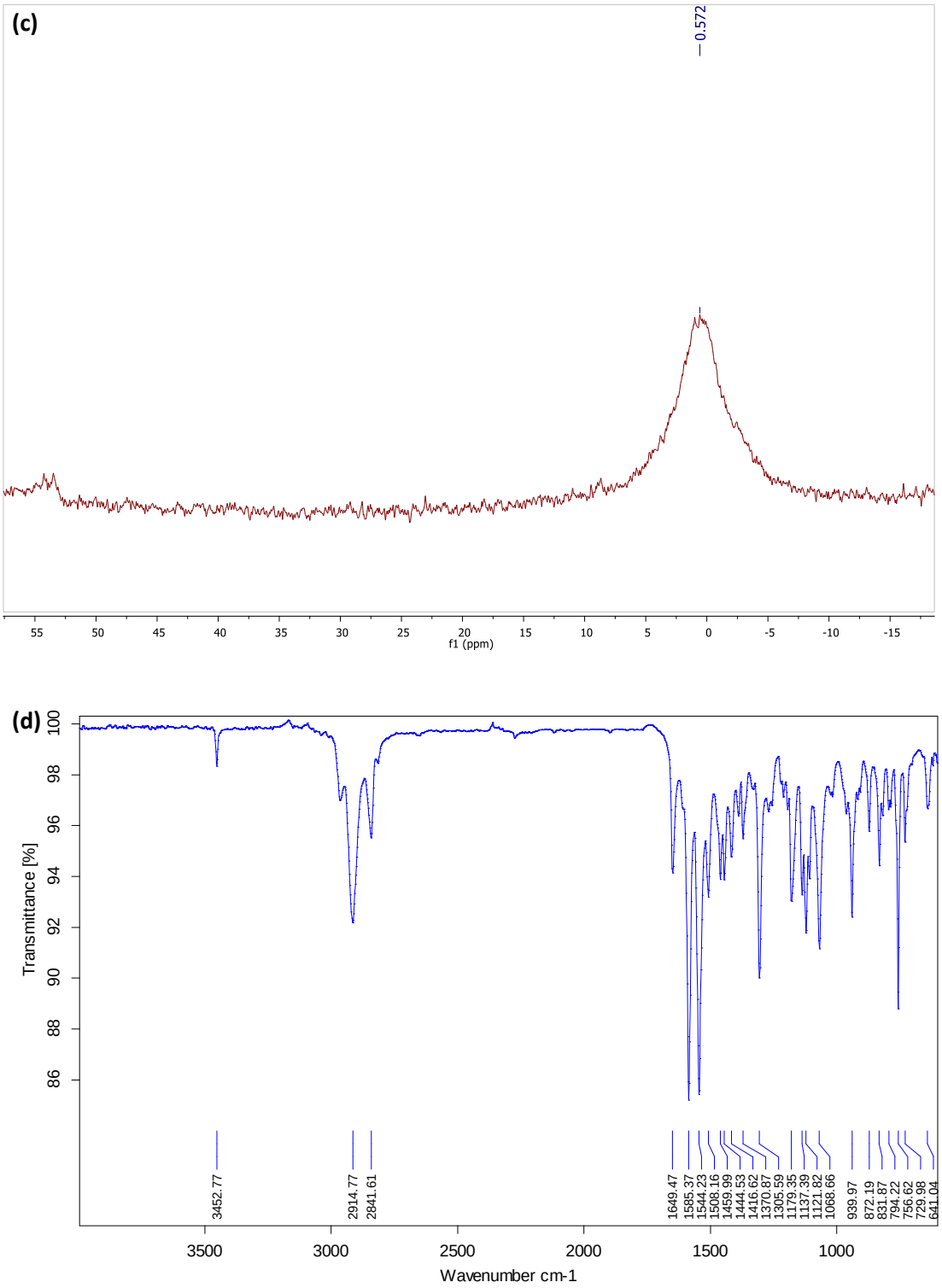

Figure S14. ^{1}H (a), $^{13}C\{^{1}H\}$ (b) NMR in C_6D_6 solution, ^{11}B NMR in tol-d_8 solution (c), and ATR-IR spectrum (d) for compound **7a**.

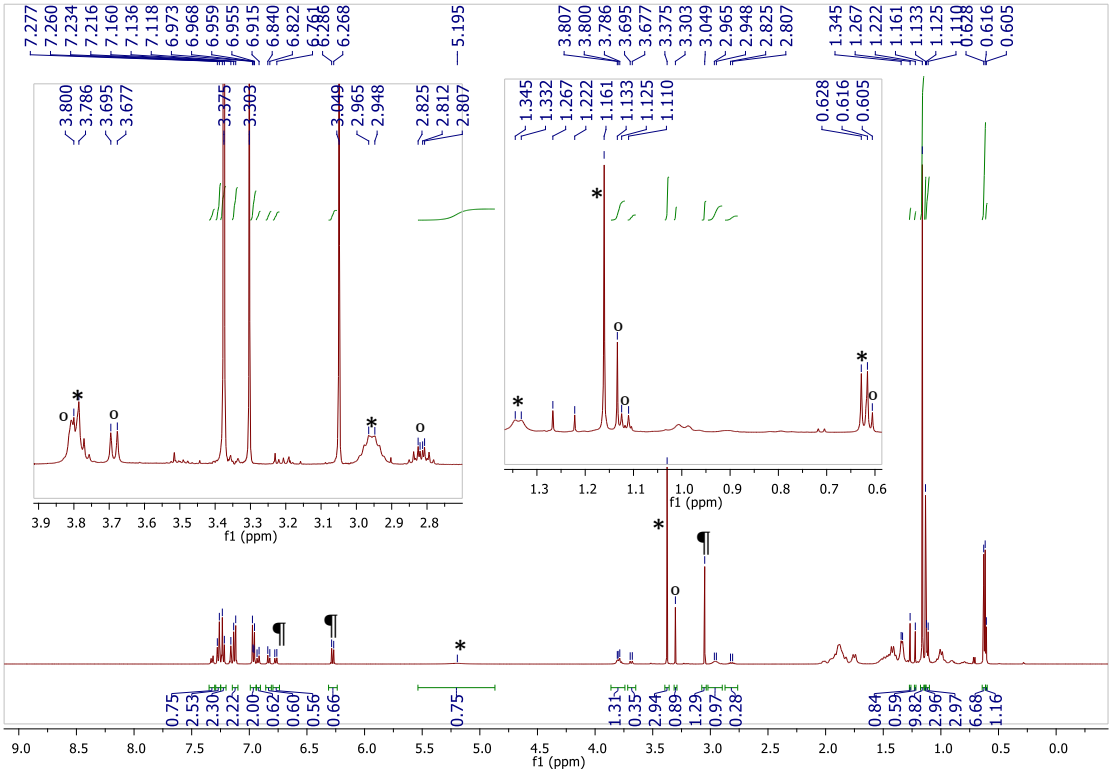

Figure S15. ^{1}H NMR spectrum in C_6D_6 solution at 298K of the reaction crude of **2** with CN(*p*-MeO-C_6H_4). * Compound **8a**; º Compound **8b**; ¶ CN(*p*-MeO-C_6H_4).

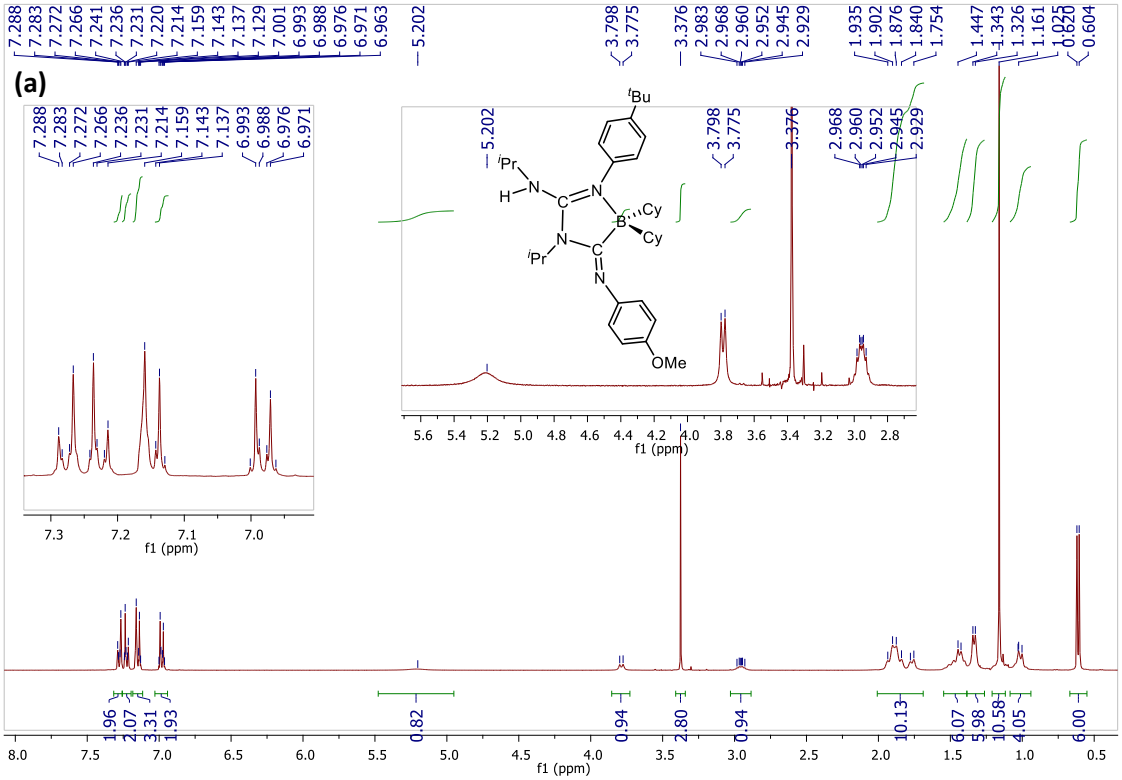
(a)
7.288
7.283
7.272
7.266
7.241
7.236
7.231
7.220
7.214
7.159
7.143
7.137
7.129
7.001
6.993
6.988
6.976
6.971
6.963
5.202
3.798
3.775
3.376
2.983
2.968
2.960
2.952
2.945
2.929
1.935
1.902
1.876
1.840
1.754
1.447
1.343
1.326
1.161
0.825
0.820
0.604
tBu
iPr
H
N
C
N
B
Cy
Cy
iPr
N
C
N
OMe
1.96
2.07
3.31
1.93
0.82
0.94
2.80
0.94
10.13
6.07
5.98
10.58
4.05
6.00
f1 (ppm)

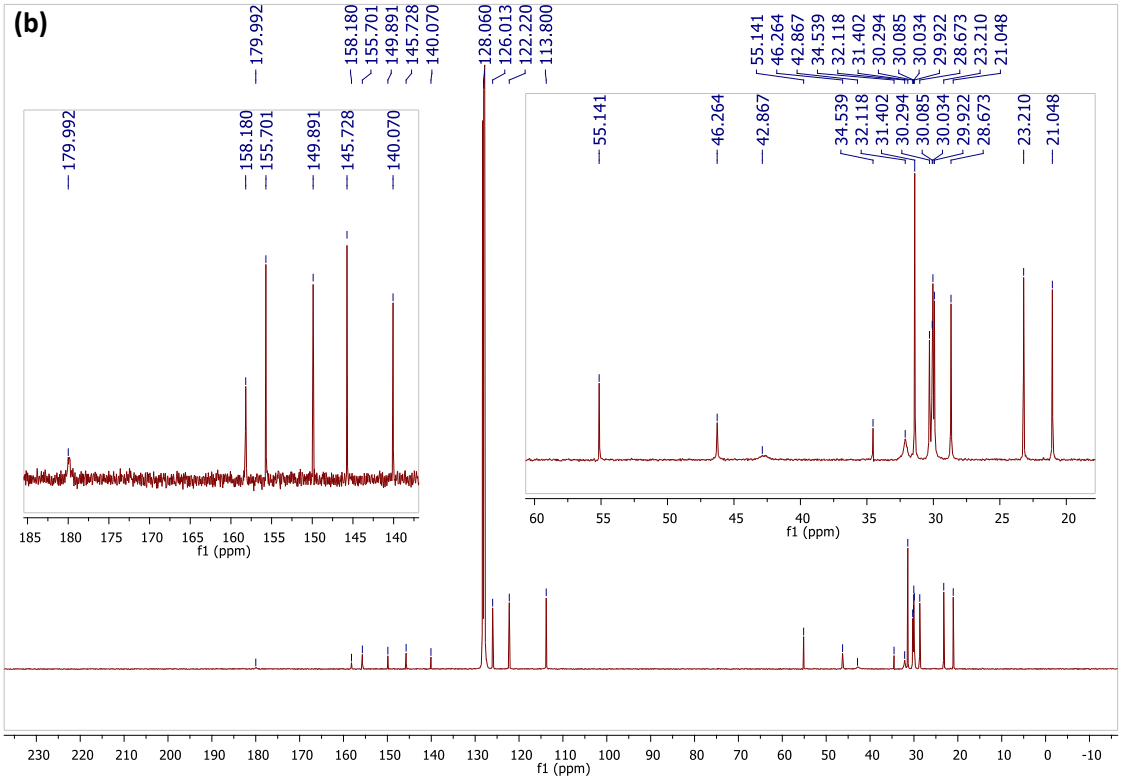
(b)
179.992
158.180
155.701
149.891
145.728
140.070
128.060
126.013
122.220
113.800
55.141
46.264
42.867
34.539
32.118
31.402
30.294
30.085
30.034
29.922
28.673
23.210
21.048
f1 (ppm)

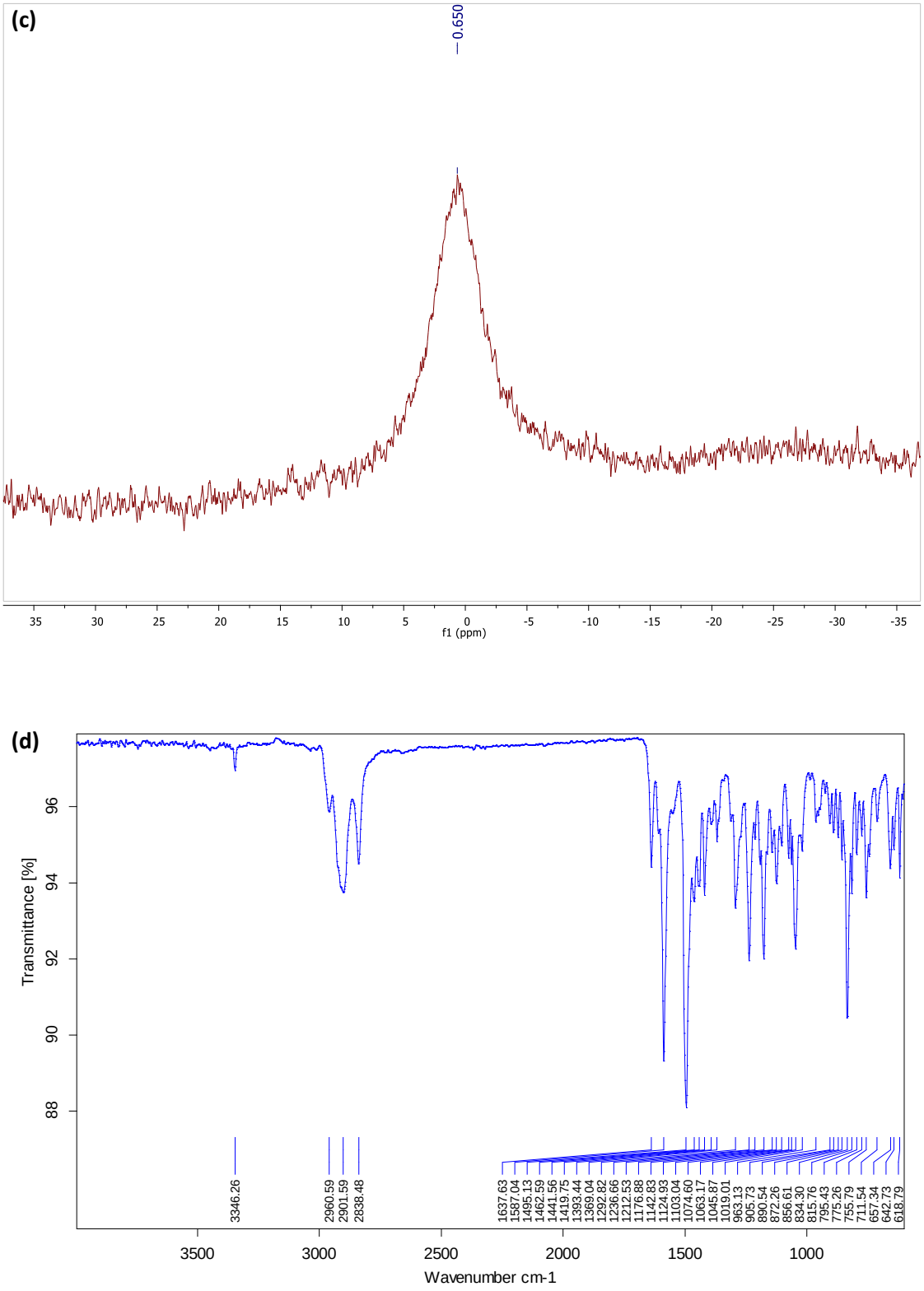

Figure S16. ^{1}H (a), $^{13}C\{^{1}H\}$ (b) NMR in C_6D_6 solution, ^{11}B NMR in tol-d_8 solution (c), and ATR-IR spectrum (d) for compound **8a**.

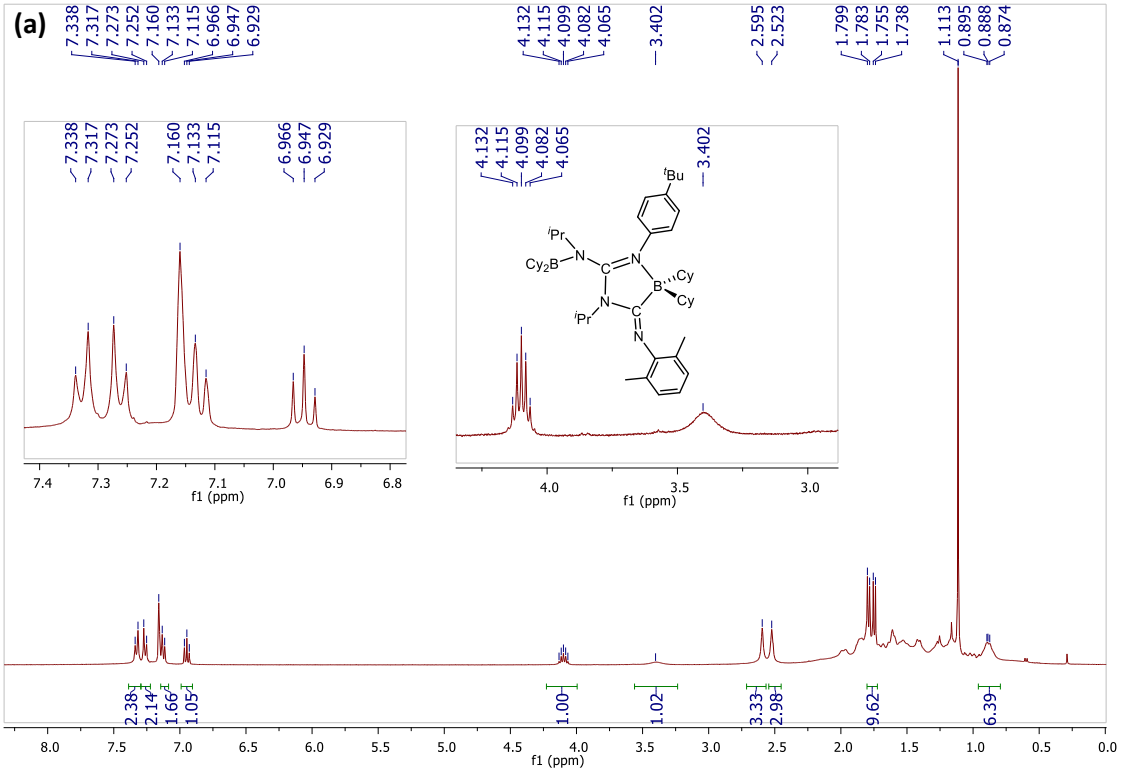
(a)
7.338
7.317
7.273
7.252
7.160
7.133
7.115
6.966
6.947
6.929
4.132
4.115
4.099
4.082
4.065
3.402
2.595
2.523
1.799
1.783
1.755
1.738
1.113
0.895
0.888
0.874
tBu
iPr
Cy2B
N
C
N
B
Cy
Cy
iPr
N
C
N
2.38
2.14
1.66
1.05
1.00
1.02
3.33
2.98
9.62
6.39
f1 (ppm)

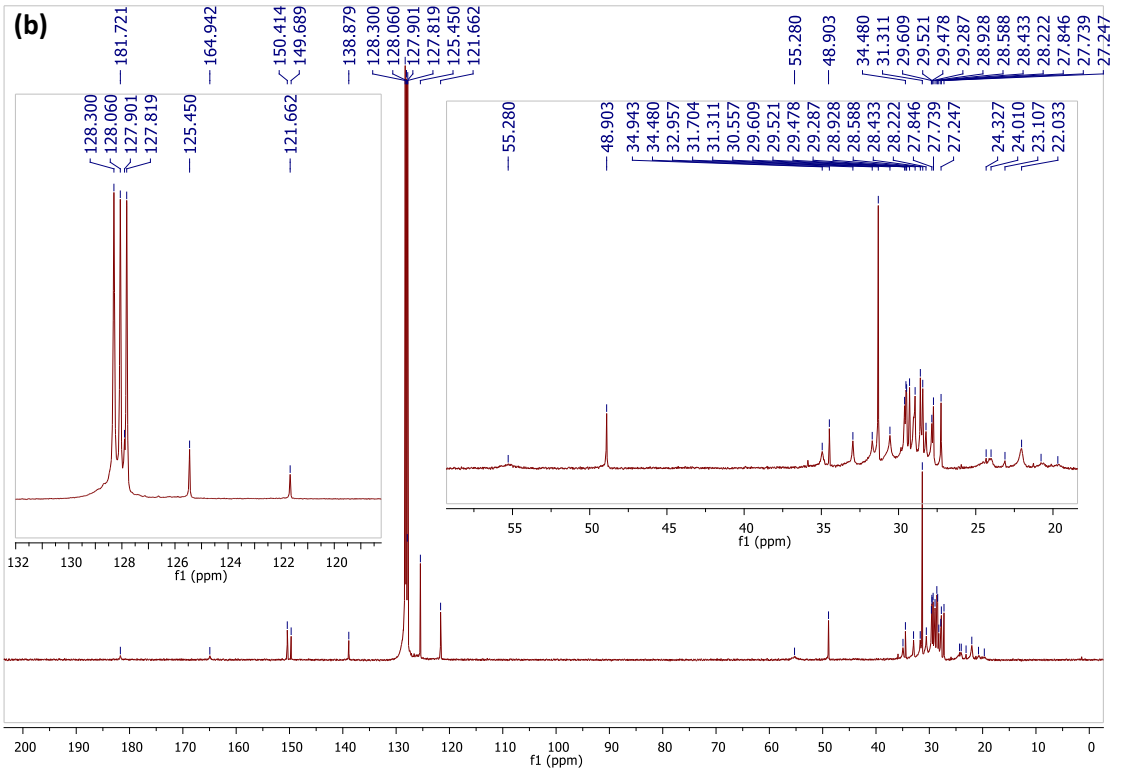
(b)
181.721
164.942
150.414
149.689
138.879
128.300
128.060
127.901
127.819
125.450
121.662
55.280
48.903
34.480
31.311
29.609
29.521
29.478
29.287
28.928
28.588
28.433
28.222
27.846
27.739
27.247
f1 (ppm)

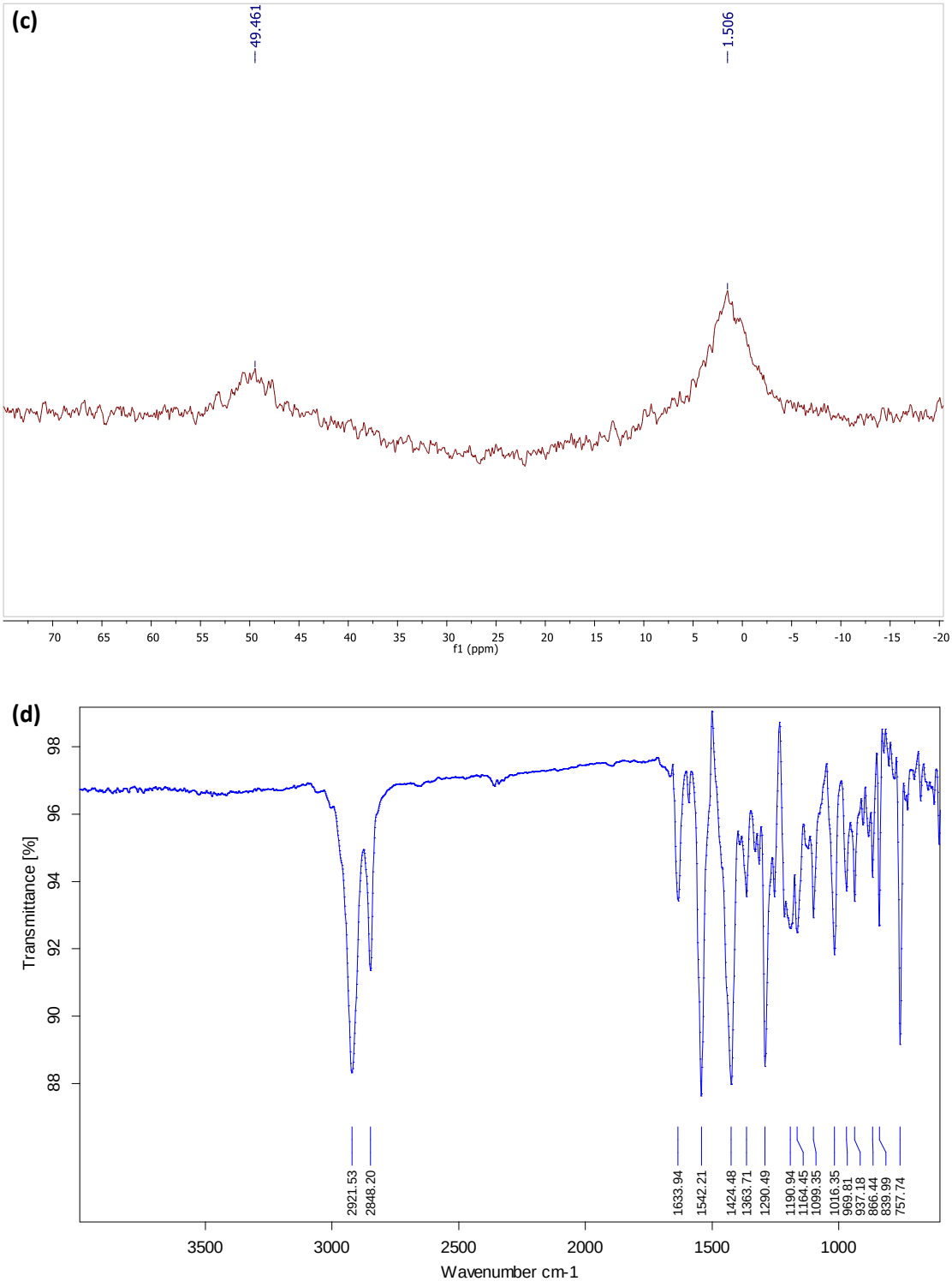

Figure S17. ^{1}H (a), $^{13}C\{^{1}H\}$ (b) NMR in C_6D_6 solution, ^{11}B NMR in tol-d_8 solution (c), and ATR-IR spectrum (d) for compound **9**.

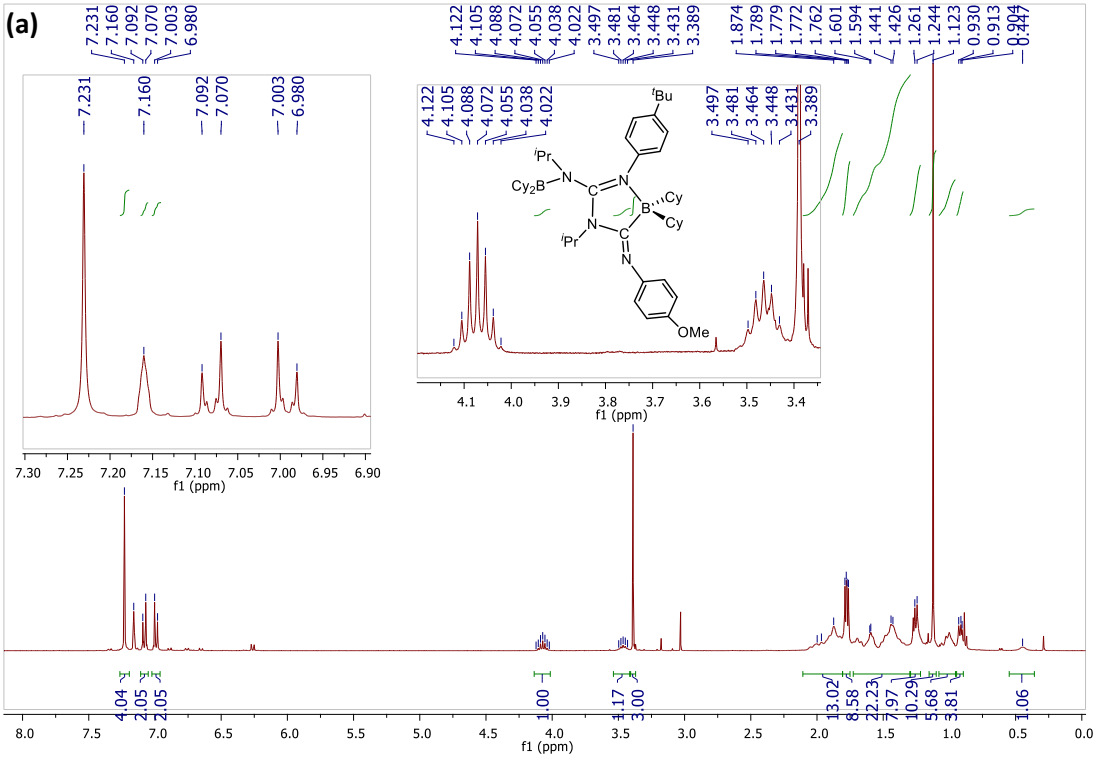
(a)
f1 (ppm)

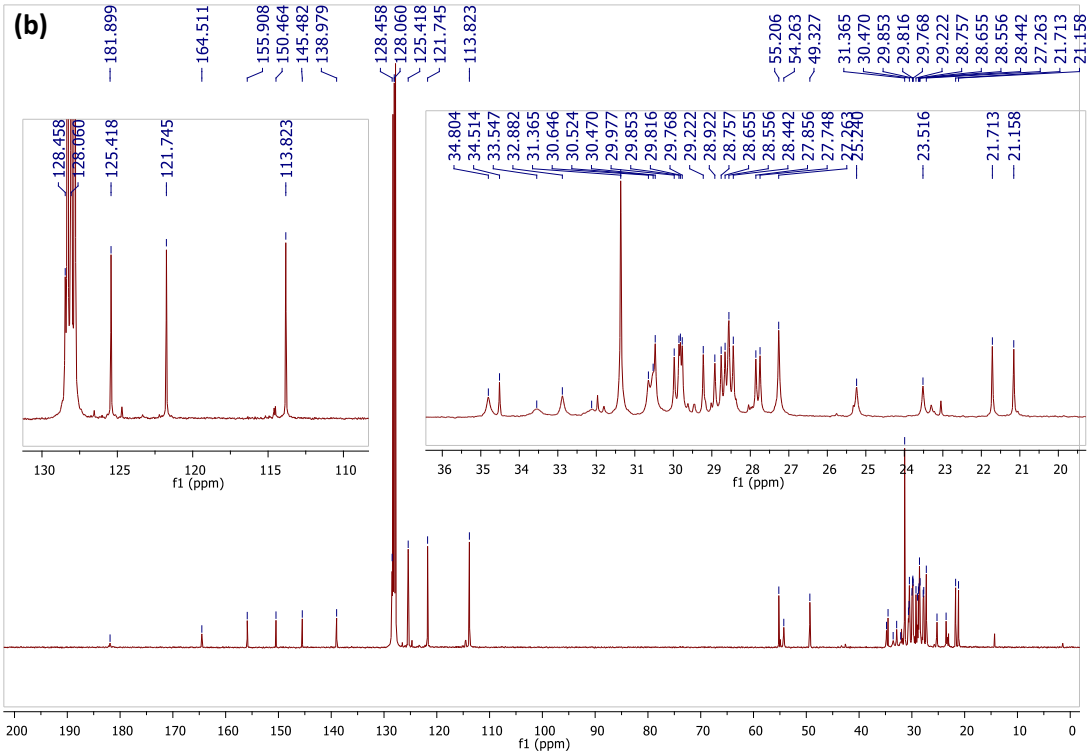
(b)
f1 (ppm)

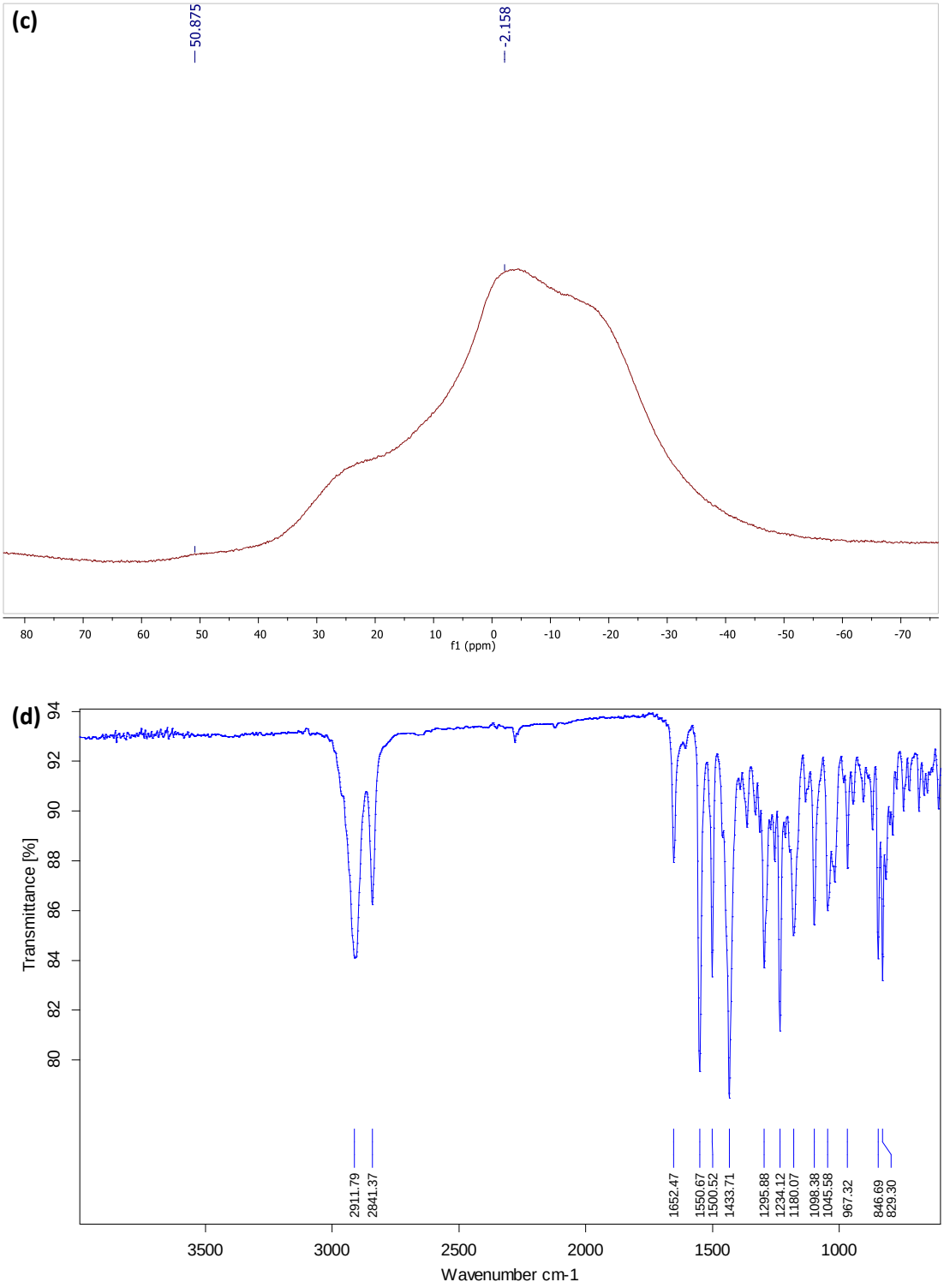

Figure S18. ^{1}H (a), $^{13}C\{^{1}H\}$ (b) and ^{11}B (c) NMR spectra in C_6D_6 solution, and ATR-IR spectrum (d) for compound **10**.

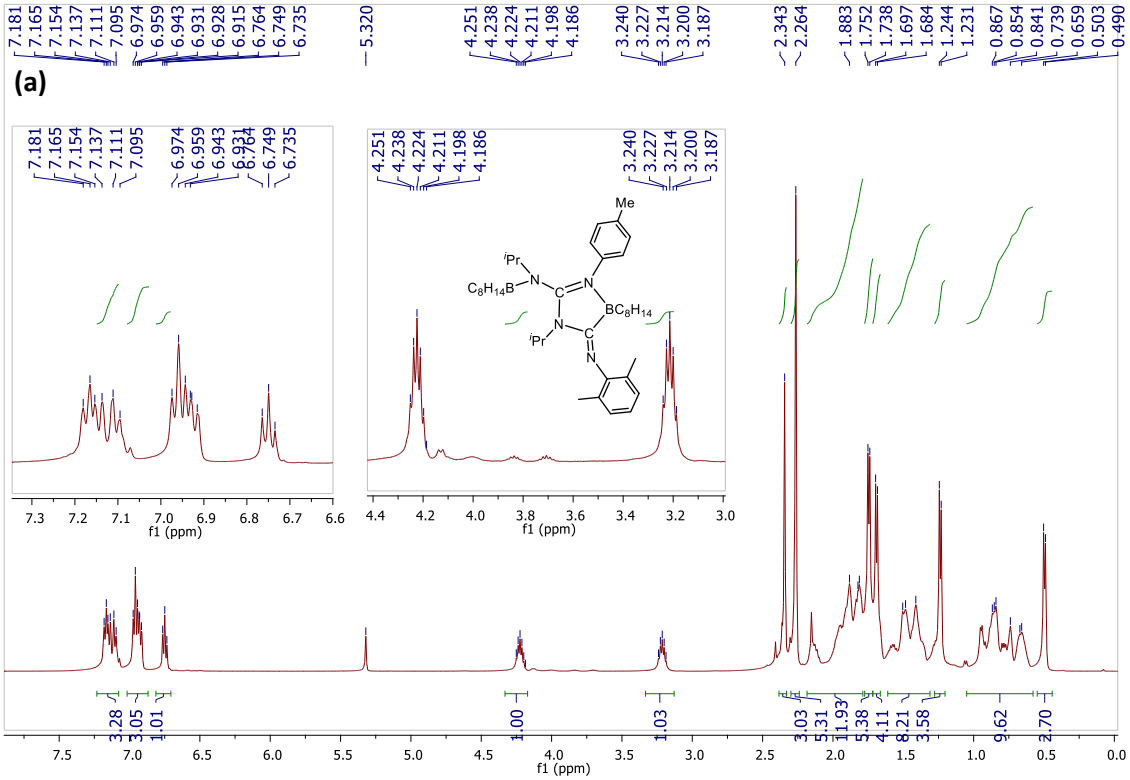
(a)
f1 (ppm)

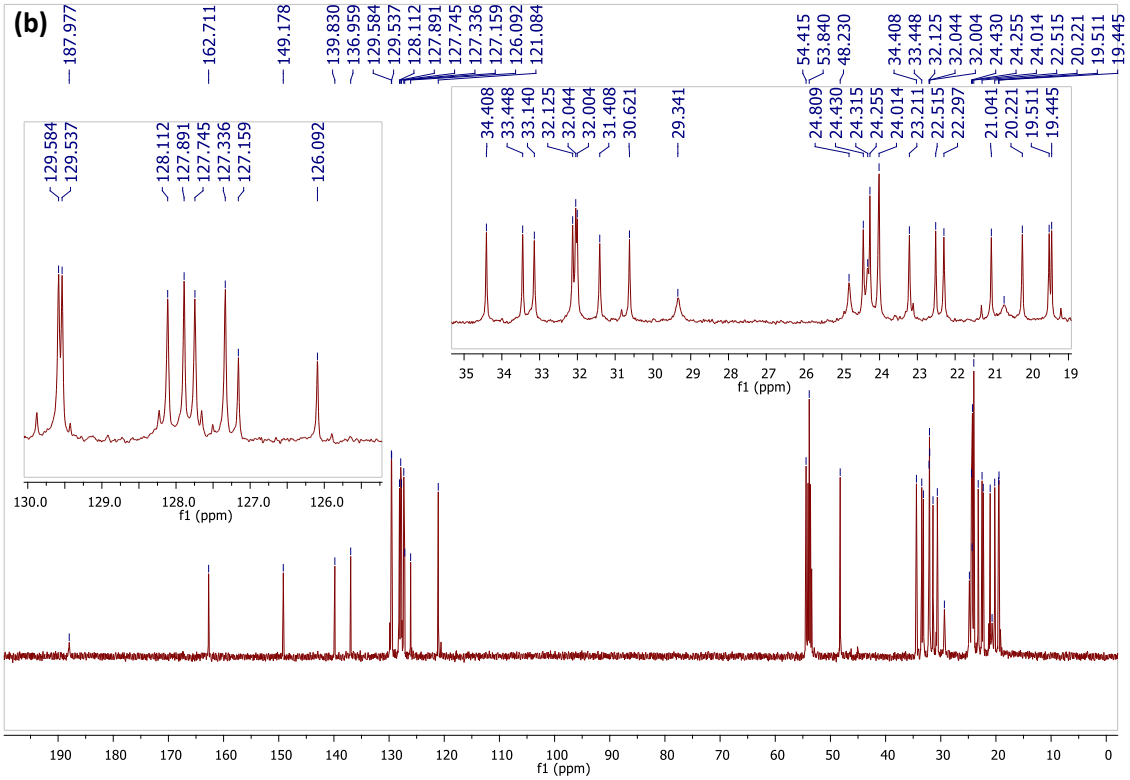
(b)
f1 (ppm)

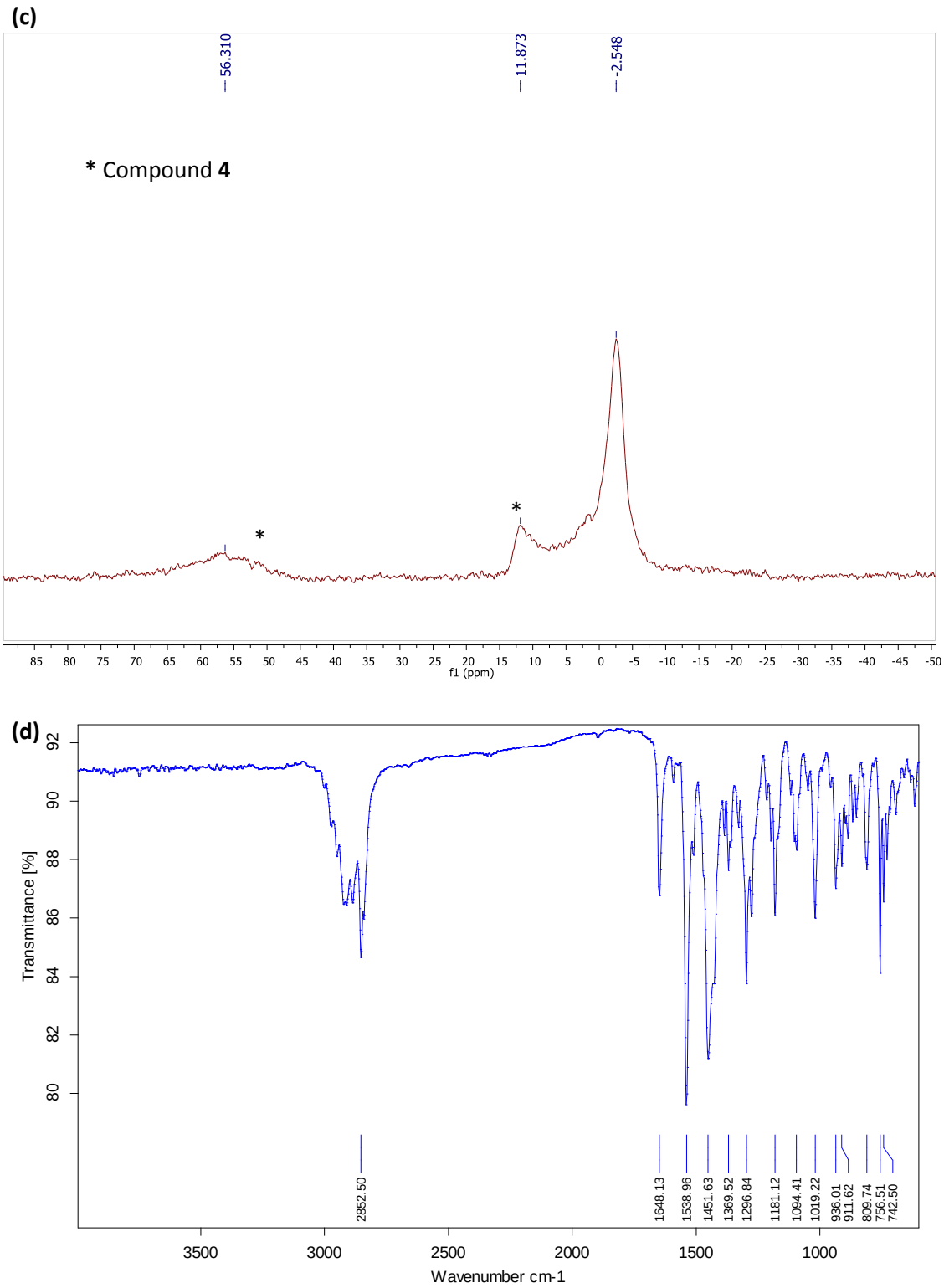

Figure S19. ^{1}H (a), $^{13}C\{^{1}H\}$ (b) NMR at 253 K, ^{11}B NMR at 298 K (c), in CD_2Cl_2 solution, and ATR-IR spectrum (d) for compound **11**.

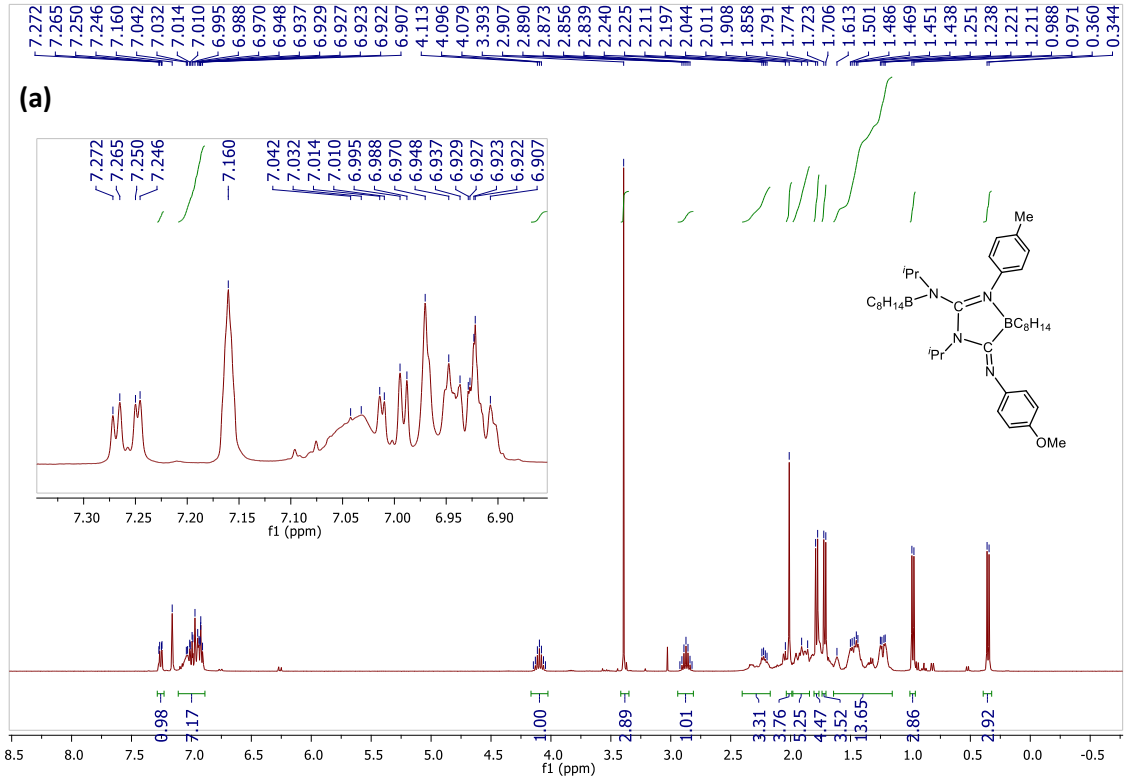
(a)
Me
OMe
f1 (ppm)

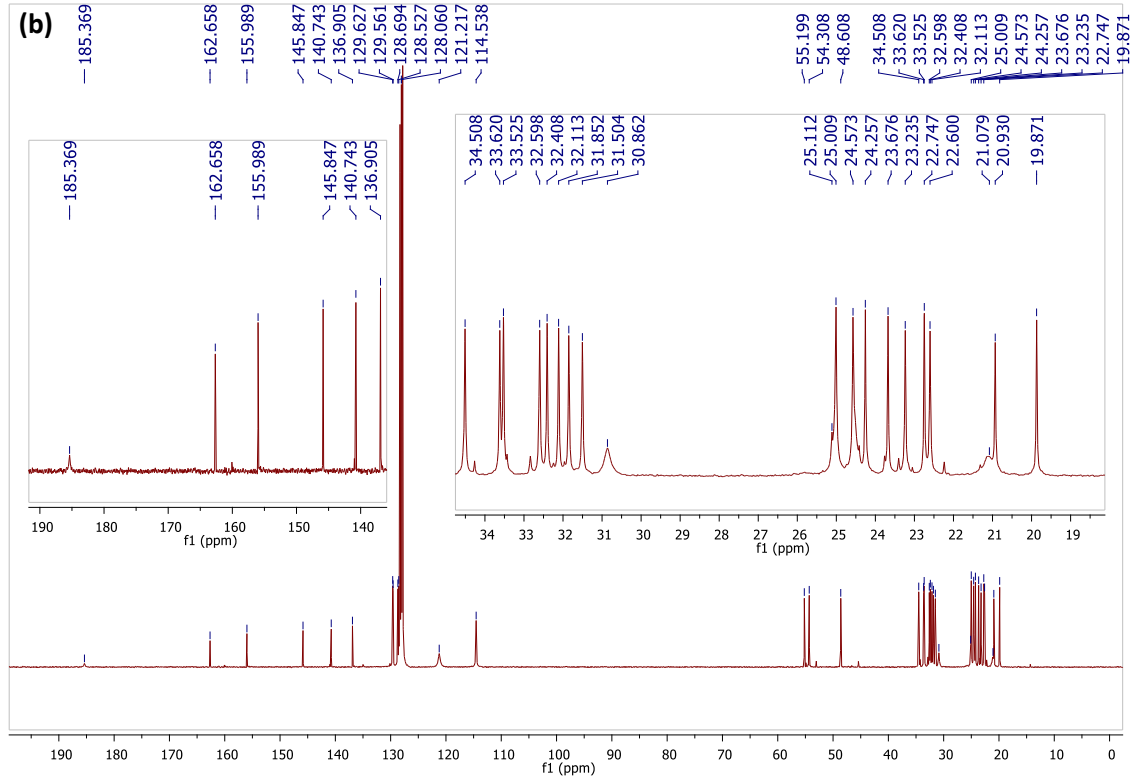
(b)
f1 (ppm)

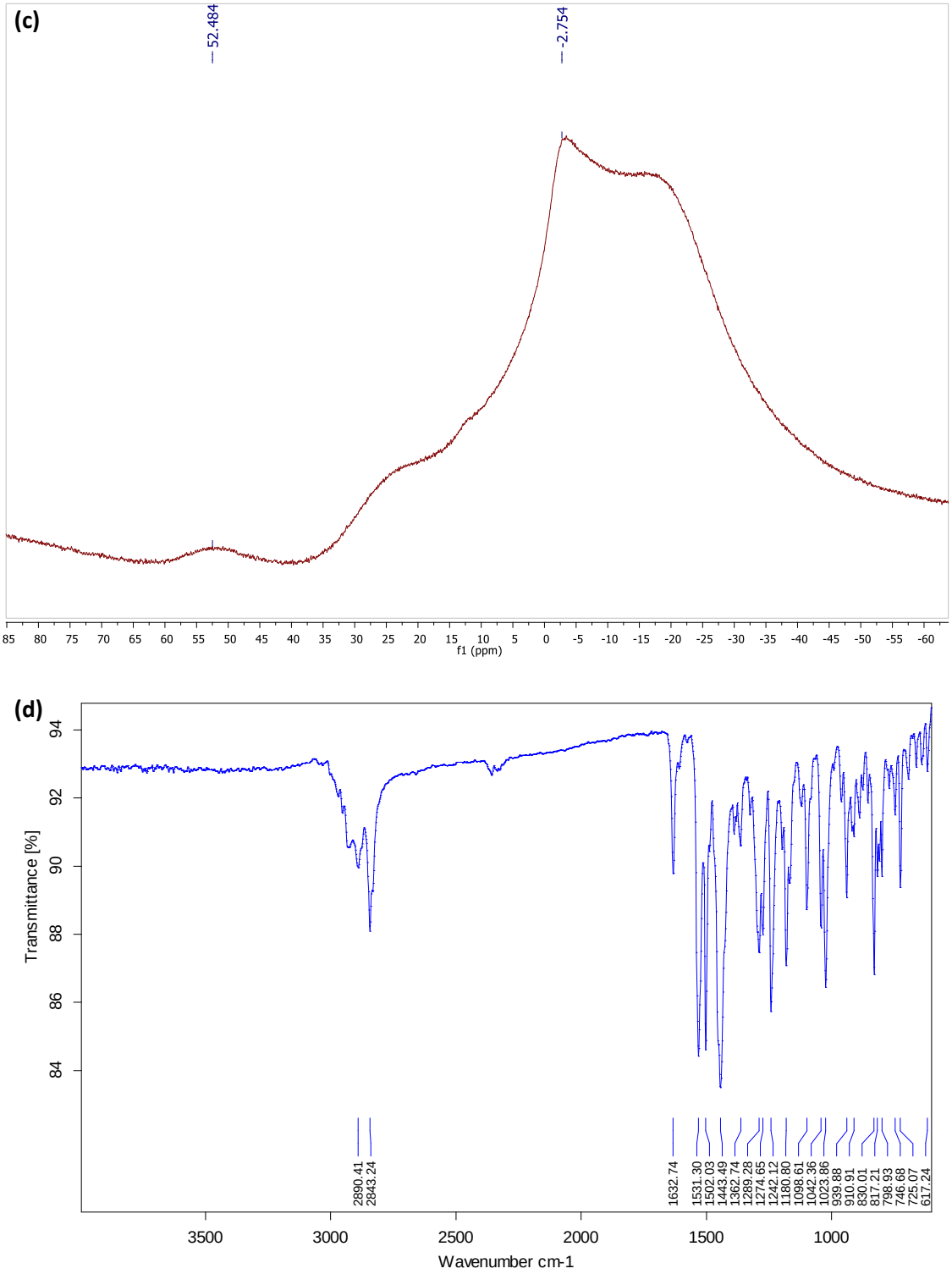

Figure S20. ^{1}H (a), $^{13}C\{^{1}H\}$ (b) and ^{11}B (c) NMR spectra in C_6D_6 solution, and ATR-IR spectrum (d) for compound **12**.

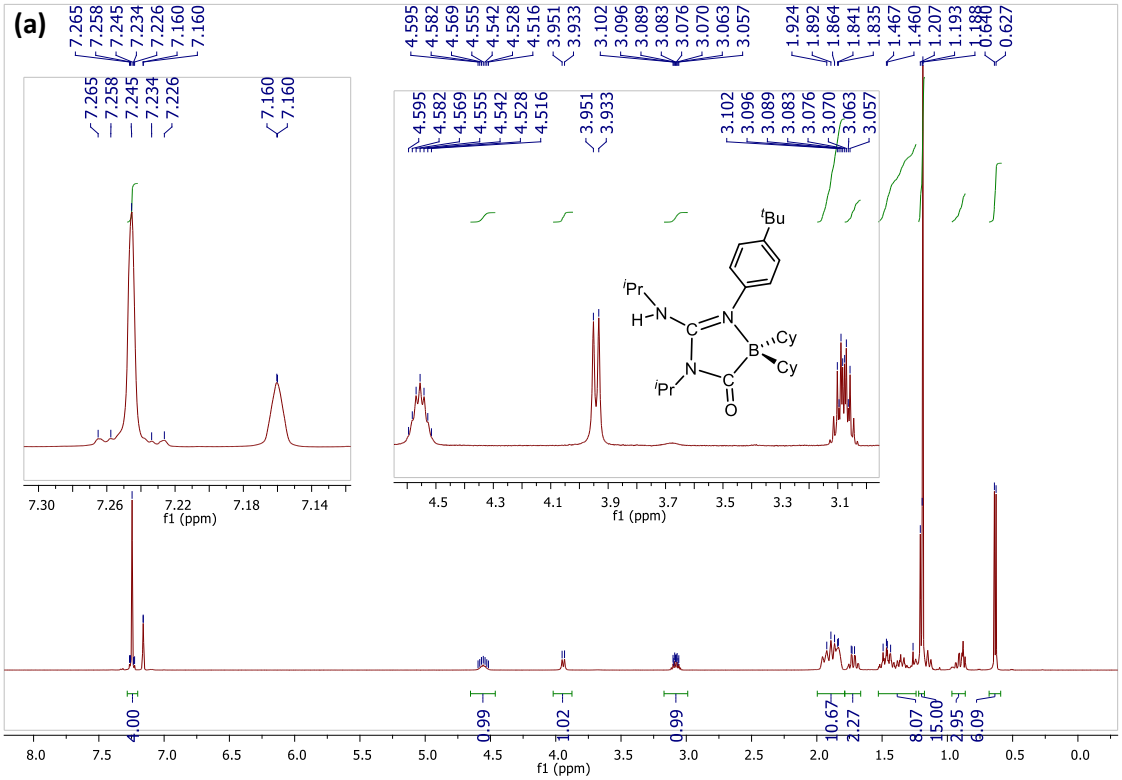
(a)
7.265
7.258
7.245
7.234
7.226
7.160
7.160
4.595
4.582
4.569
4.555
4.542
4.528
4.516
3.951
3.933
3.102
3.096
3.089
3.083
3.076
3.070
3.063
3.057
1.924
1.892
1.864
1.841
1.835
1.467
1.460
1.207
1.193
0.640
0.627
tBu
iPr
H-N
C
N
B
Cy
Cy
iPr
N
C
O
f1 (ppm)
4.00
0.99
1.02
0.99
10.67
2.27
8.07
15.00
2.95
6.09

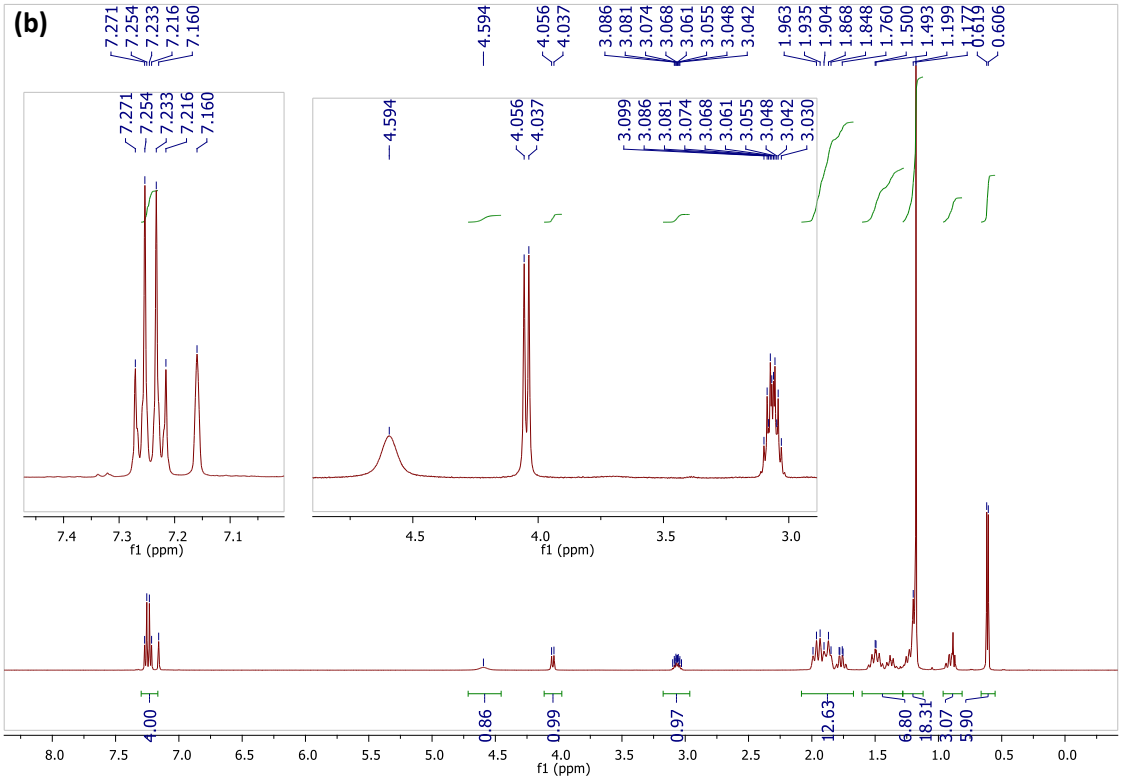
(b)
7.271
7.254
7.233
7.216
7.160
4.594
4.056
4.037
3.086
3.081
3.074
3.068
3.061
3.055
3.048
3.042
1.963
1.935
1.904
1.868
1.848
1.760
1.500
1.493
1.199
0.606
3.099
3.030
f1 (ppm)
4.00
0.86
0.99
0.97
12.63
6.80
18.31
3.07
5.90

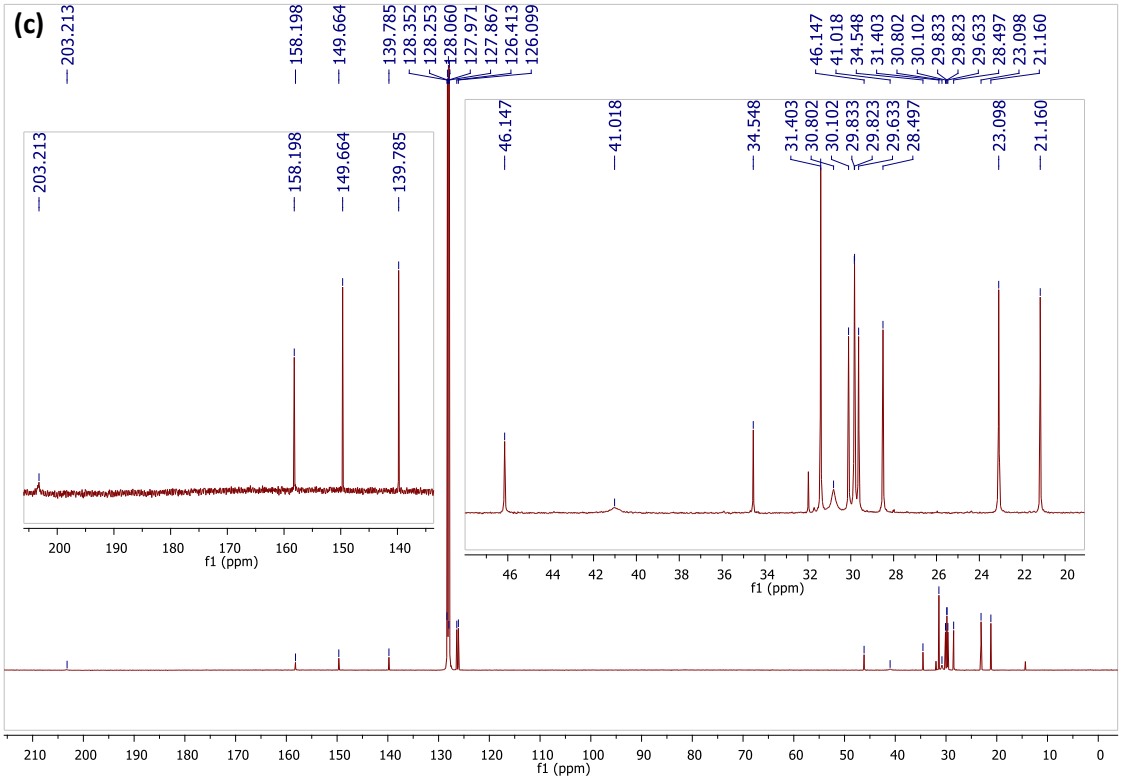
(c)
203.213
158.198
149.664
139.785
128.352
128.253
128.060
127.971
127.867
126.413
126.099
46.147
41.018
34.548
31.403
30.802
30.102
29.833
29.823
29.633
28.497
23.098
21.160
f1 (ppm)

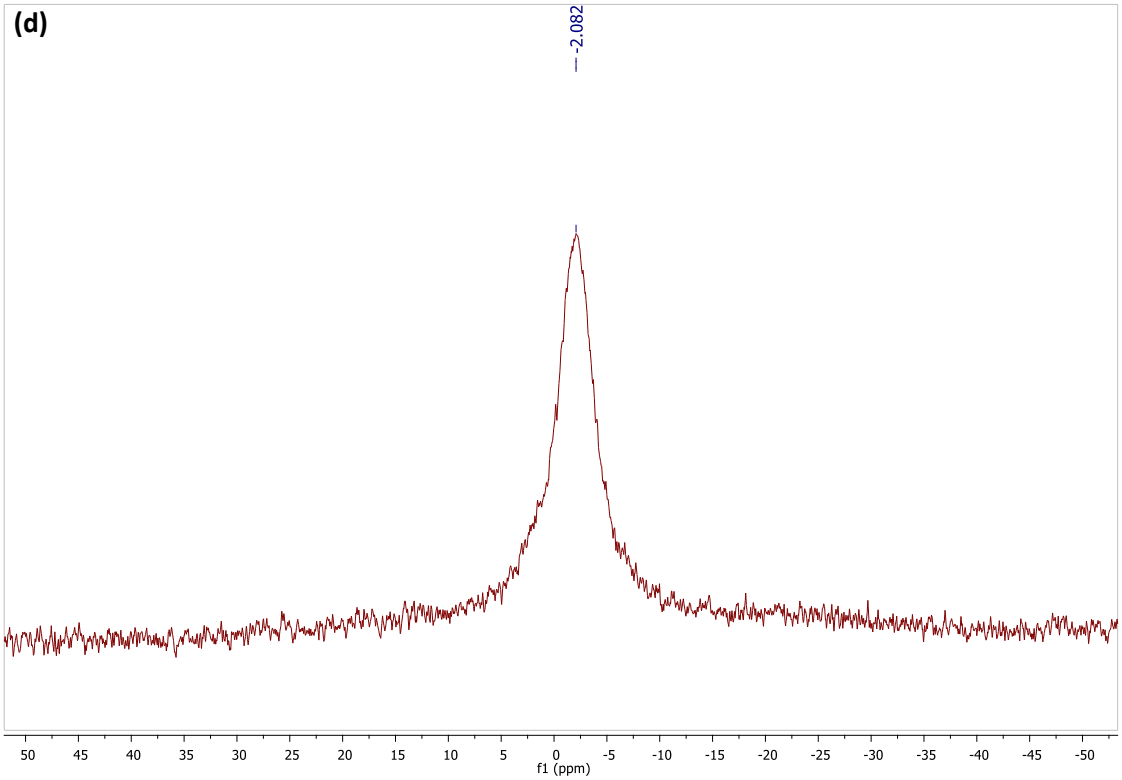
(d)
-2.082
f1 (ppm)

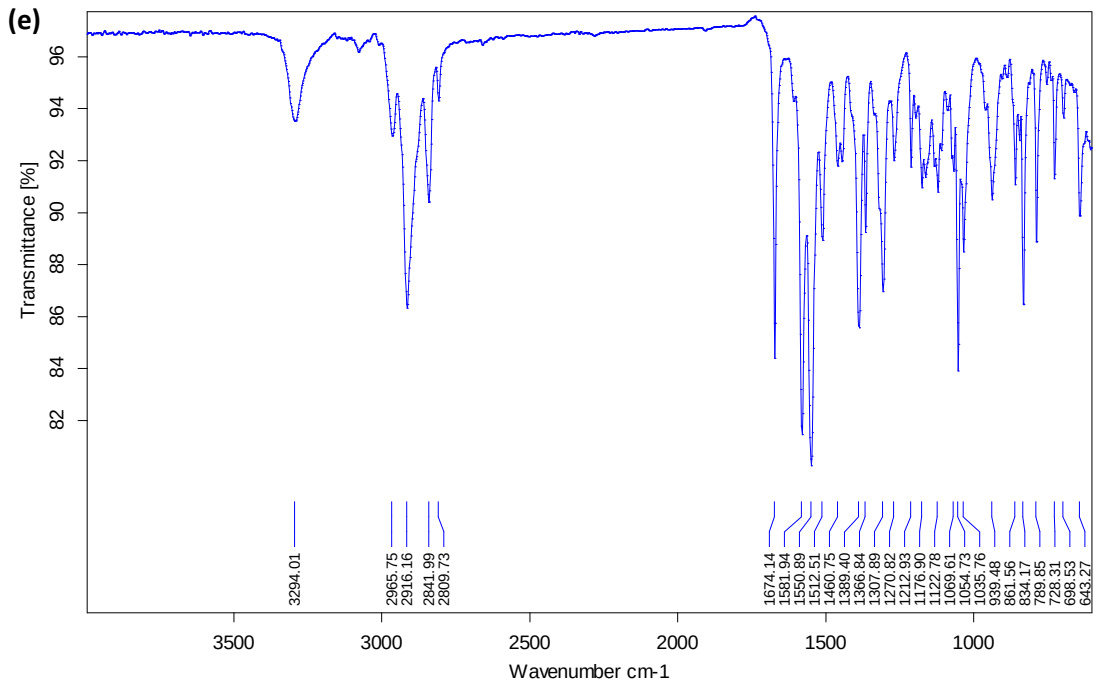

Figure S21. ^{1}H NMR at 333 K (a), ^{1}H (b), ^{13}C{^{1}H} (c), ^{11}B (d) NMR at 298 K, in C_6D_6 solution, and ATR-IR spectrum (e) for compound **13**.

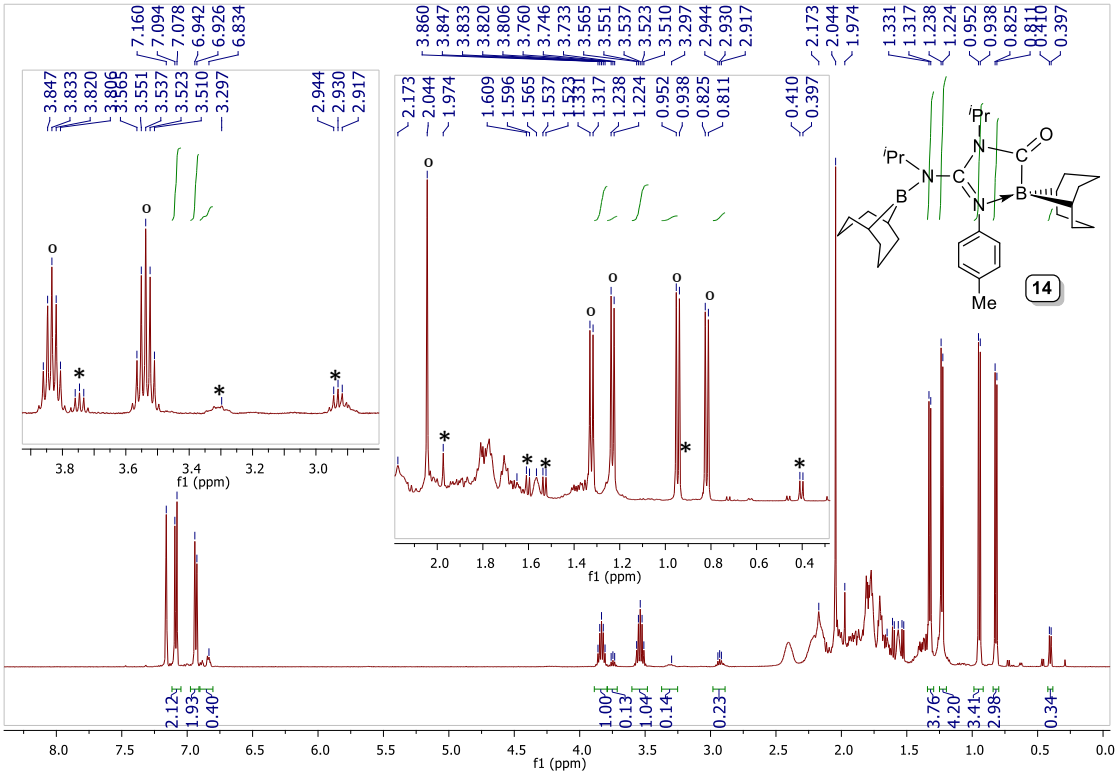

Figure S22. ^{1}H NMR spectrum in C_6D_6 solution at 298 K of the reaction crude of **4** with CO. [* Compound **14**; º Compound **4**.]

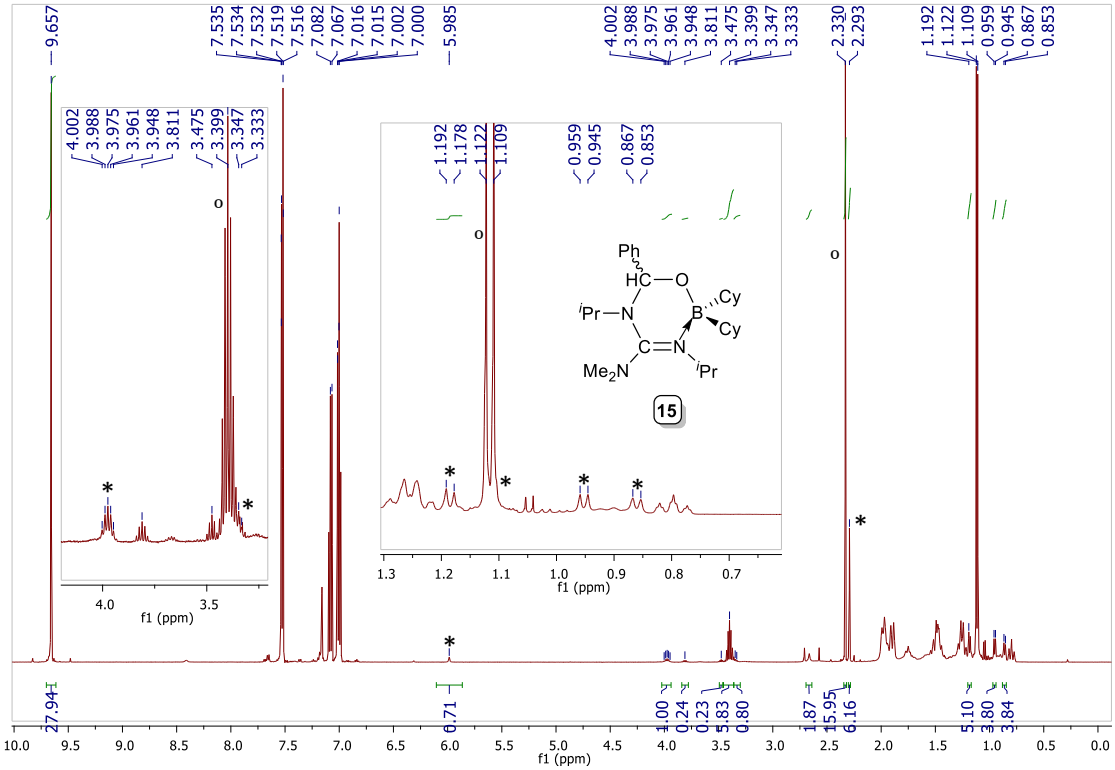

Figure S23. ^{1}H NMR spectrum in C_6D_6 solution at 298 K of the reaction crude of **1** with benzaldehyde. [* Compound **15**; º Compound **1**.]

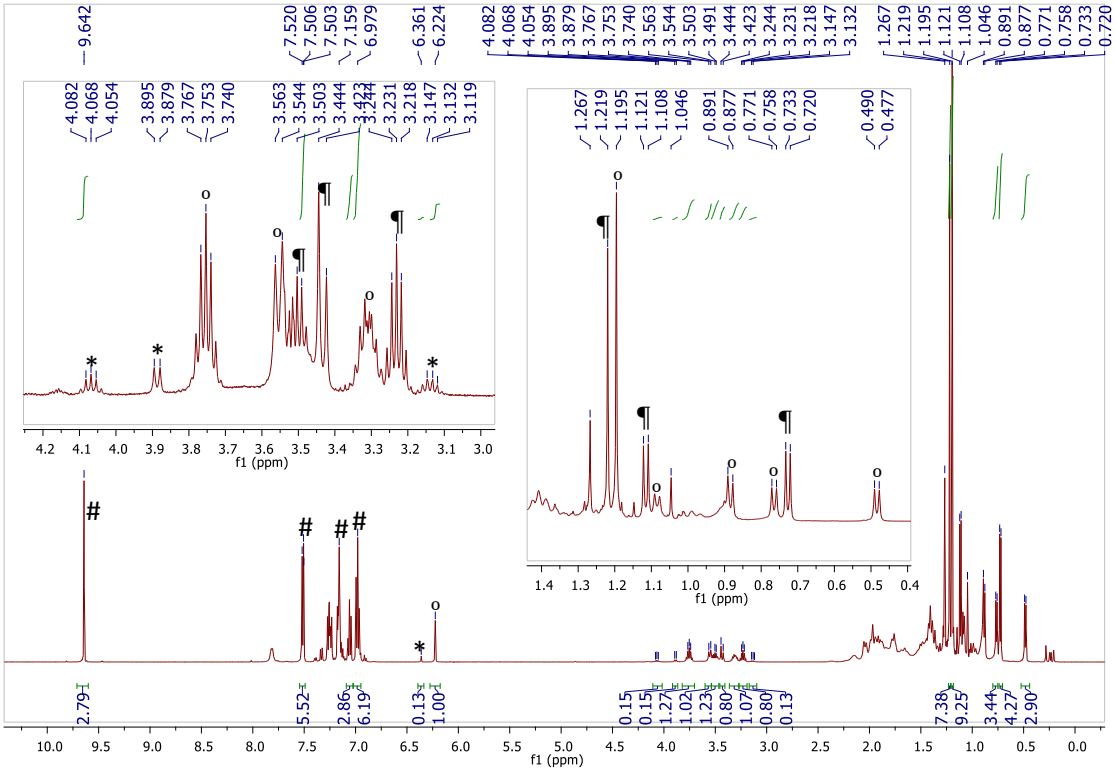

Figure S24. ^{1}H NMR spectrum in C_6D_6 solution at 298 K of the reaction crude of **2** with benzaldehyde. [º Compound **16a**; * Compound **16b**; ¶ Compound **2**; # Benzaldehyde.]

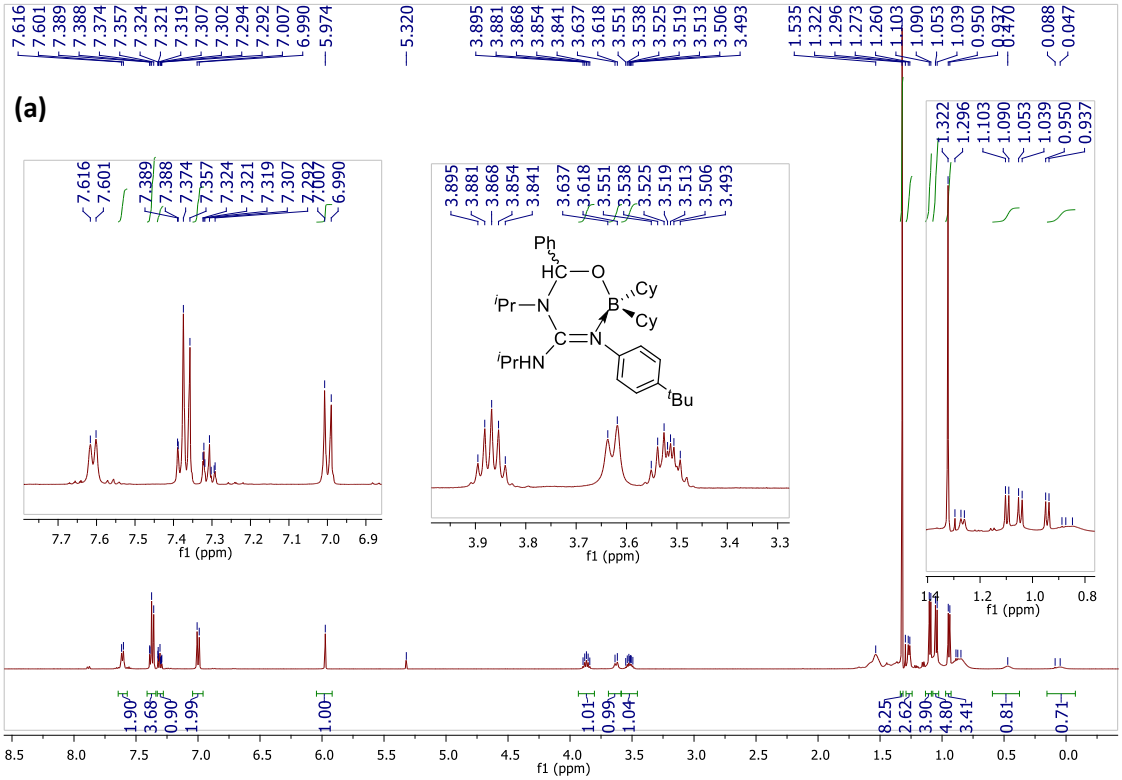
(a)
Ph
HC—O
iPr—N
B
Cy
Cy
C=N
iPrHN
tBu
f1 (ppm)

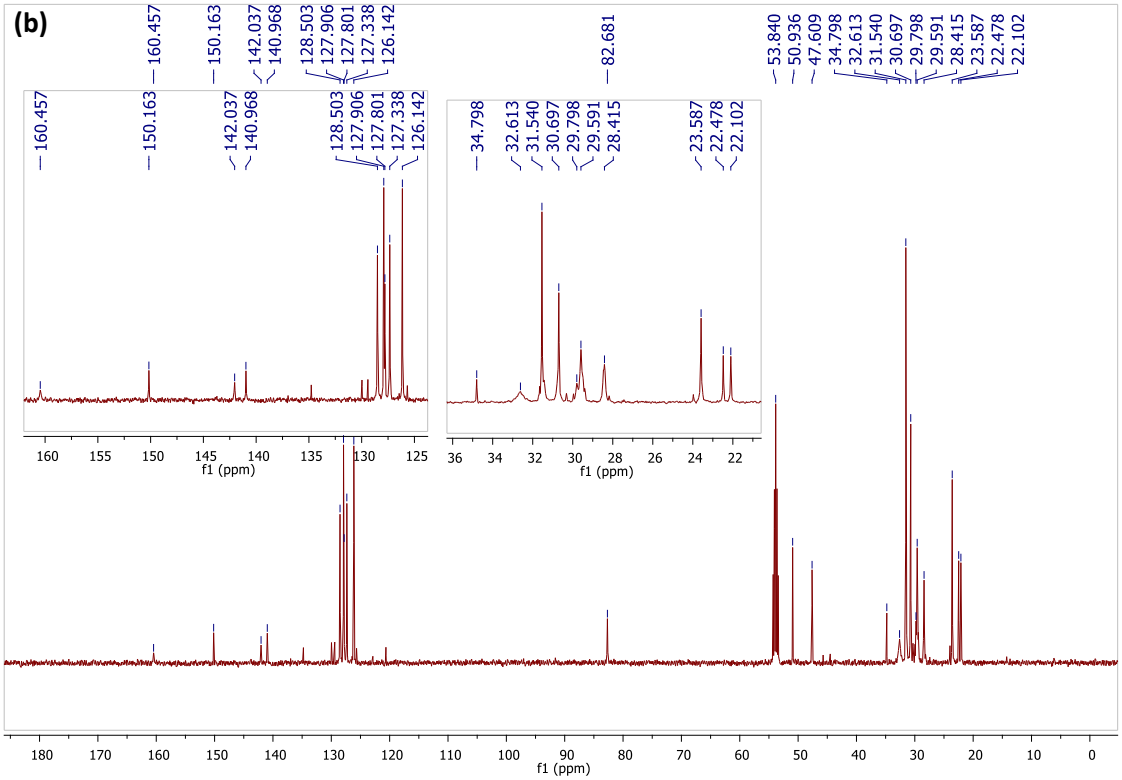
(b)
f1 (ppm)

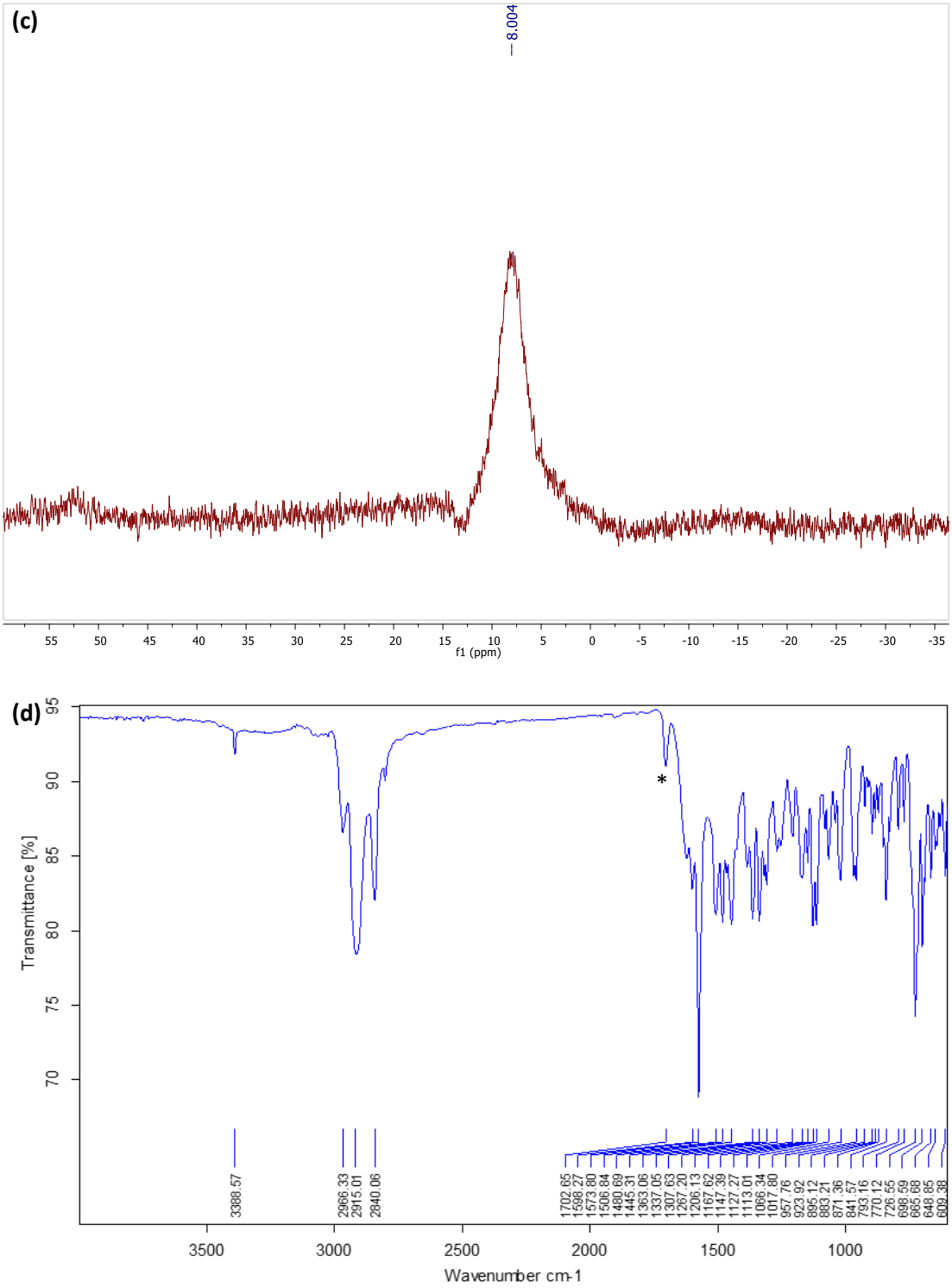

Figure S25. ^{1}H (a), $^{13}C\{^{1}H\}$ (b) and ^{11}B (c) NMR spectra in CD_2Cl_2 solution, and ATR-IR spectrum (d) for compound **16a**. [* C-O stretch from benzaldehyde]

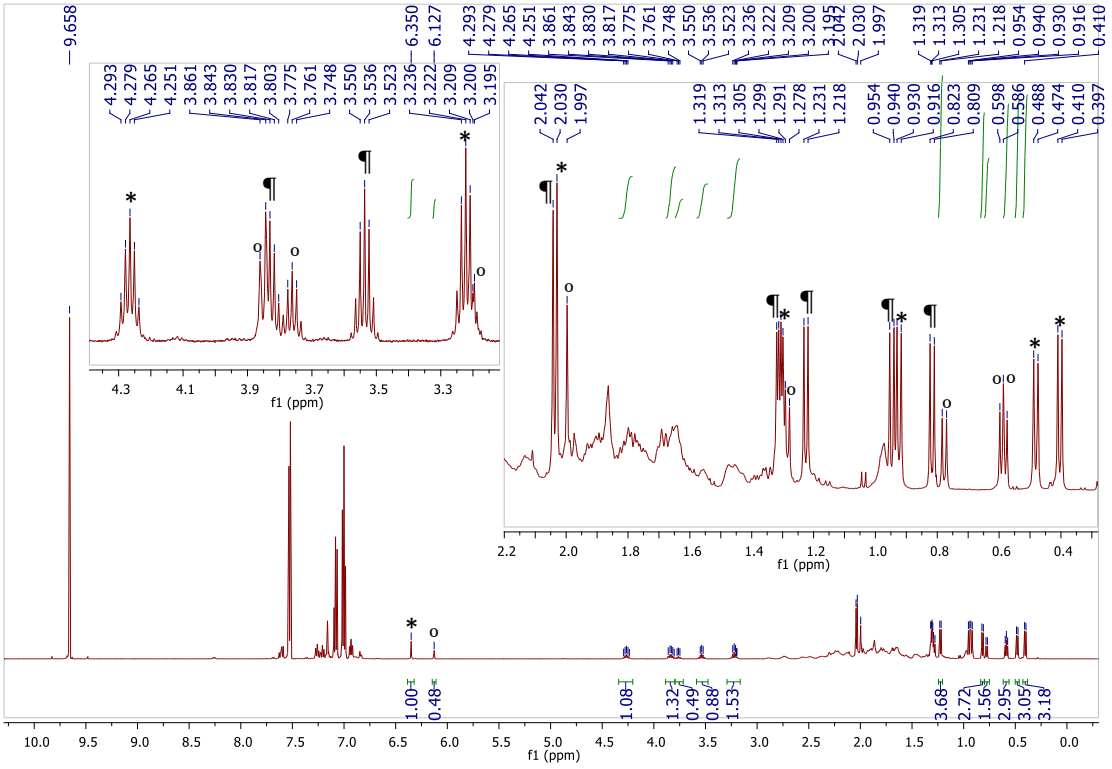

Figure S26. ^{1}H NMR spectrum in C_6D_6 solution at 298 K of the reaction crude of **4** with benzaldehyde. [* Compound **17**; º Compound **18**; ¶ Compound **4**.]

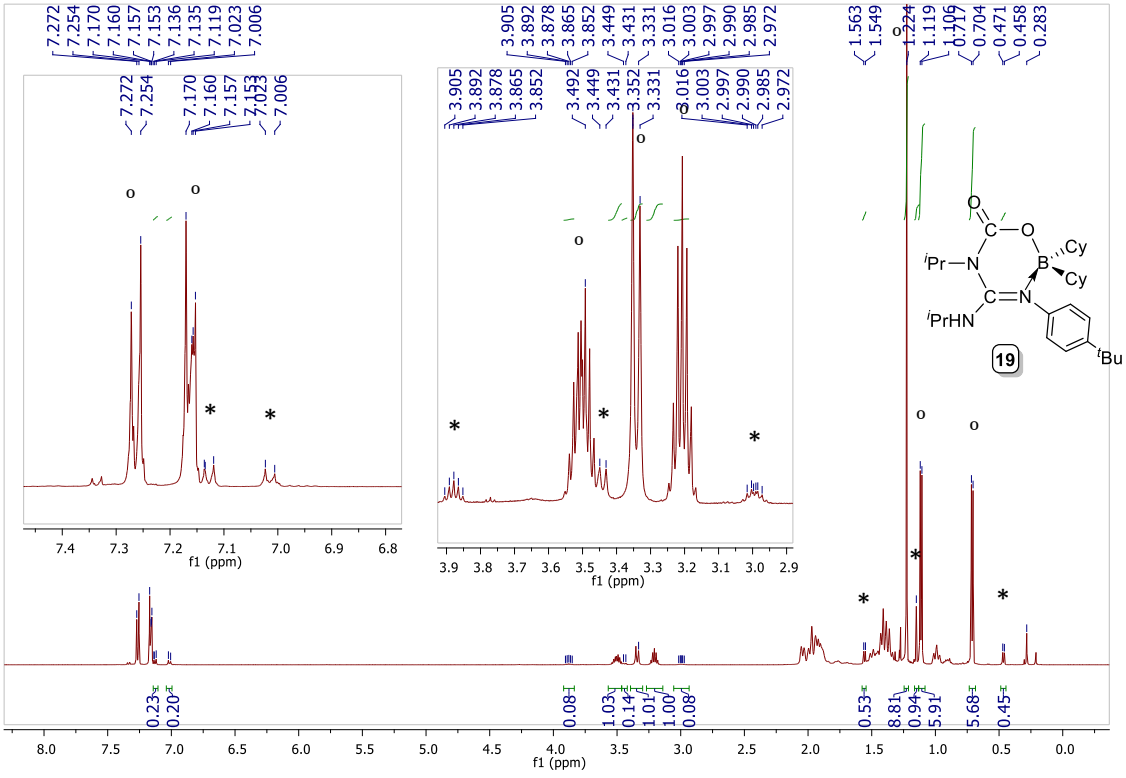

Figure S27. ^{1}H NMR spectrum in C_6D_6 solution at 298 K of the reaction crude of **2** with CO_2. [* Compound **19**; º Compound **2**.]

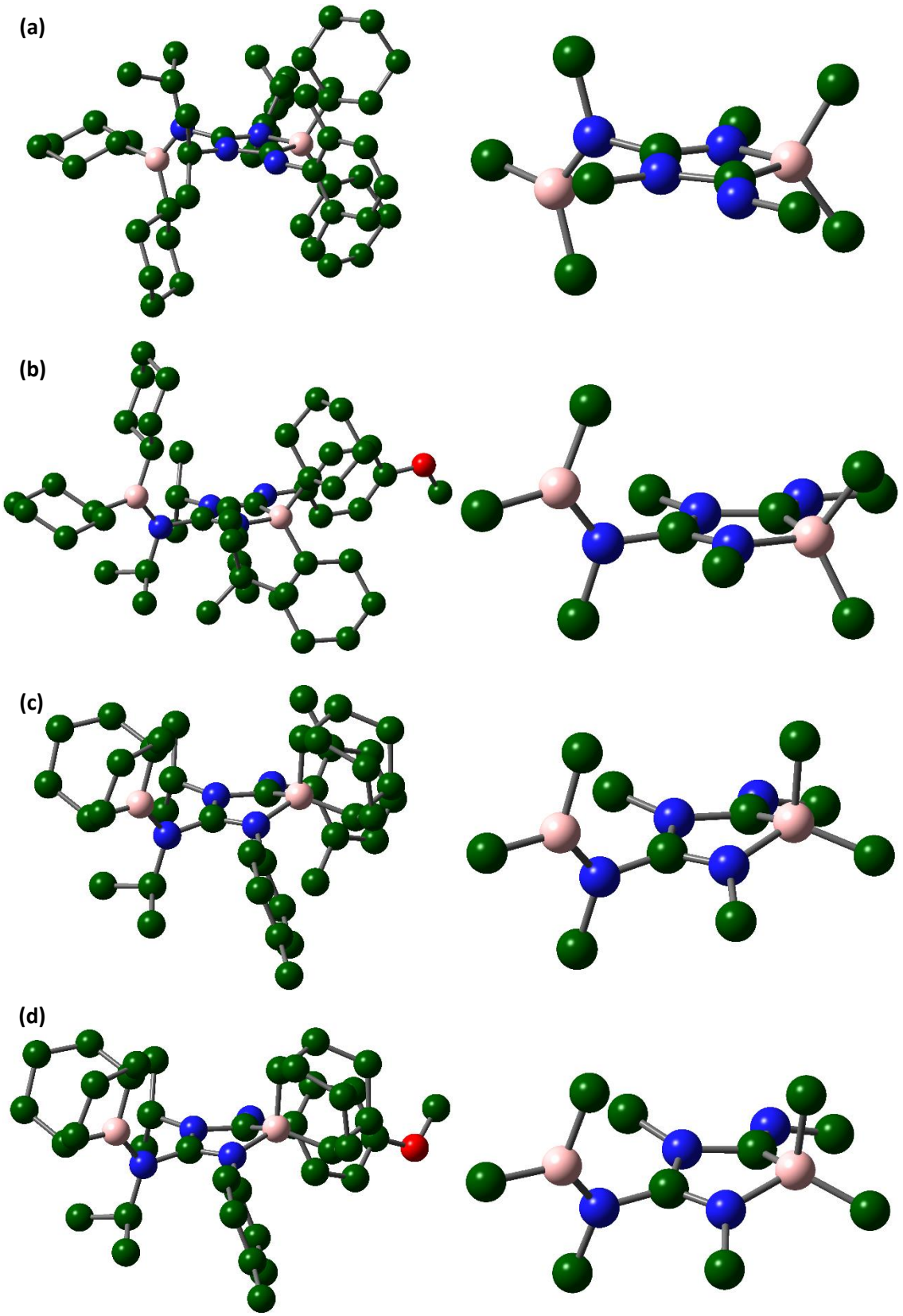

Figure S28. Optimised structures for compounds **9** (a), **10** (b), **11** (c) and **12** (d). Colour code: C, green; B, pink; N, blue; O, red. [*Left*: H atoms omitted only. *Right*: More atoms omitted to focus on heterocycle ring].

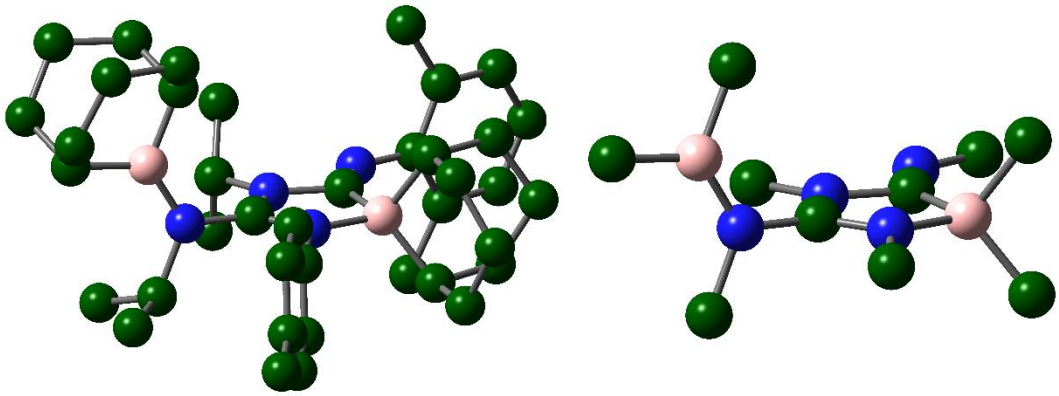

Figure S29. Optimised constrained structure for compound **11** with a planar five-membered heterocyclic ring. Colour code: C, green; B, pink; N, blue. [*Left*: H atoms omitted only. *Right*: More atoms omitted to focus on heterocycle ring].